CHAPTER 2

Stresses and Strains in Flexible Pavements

2.1 HOMOGENEOUS MASS

The simplest way to characterize the behavior of a flexible pavement under wheel loads is to consider it as a homogeneous half-space. A half-space has an infinitely large area and an infinite depth with a top plane on which the loads are applied. The original Boussinesq (1885) theory was based on a concentrated load applied on an elastic half-space. The stresses, strains, and deflections due to a concentrated load can be integrated to obtain those due to a circular loaded area. Before the development of layered theory by Burmister (1943), much attention was paid to Boussinesq solutions because they were the only ones available. The theory can be used to determine the stresses, strains, and deflections in the subgrade if the modulus ratio between the pavement and the subgrade is close to unity, as exemplified by a thin asphalt surface and a thin granular base. If the modulus ratio is much greater than unity, the equation must be modified, as demonstrated by the earlier Kansas design method (Kansas State Highway Commission, 1947).

Figure 2.1 shows a homogeneous half-space subjected to a circular load with a radius a and a uniform pressure q. The half-space has an elastic modulus E and a Poisson ratio v. A small cylindrical element with center at a distance z below the surface and r from the axis of symmetry is shown. Because of axisymmetry, there are only three normal stresses, σ_z, σ_r, and σ_t, and one shear stress, τ_{rz}, which is equal to τ_{zr}. These stresses are functions of q, r/a, and z/a.

2.1.1 Solutions by Charts

Foster and Ahlvin (1954) presented charts for determining vertical stress σ_z, radial stress σ_r, tangential stress σ_t, shear stress τ_{rz}, and vertical deflection w, as shown in Figures 2.2 through 2.6. The load is applied over a circular area with a radius a—and an

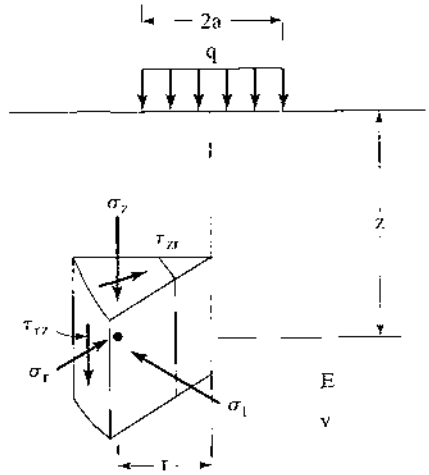

FIGURE 2.1

Component of stresses under axisymmetric loading.

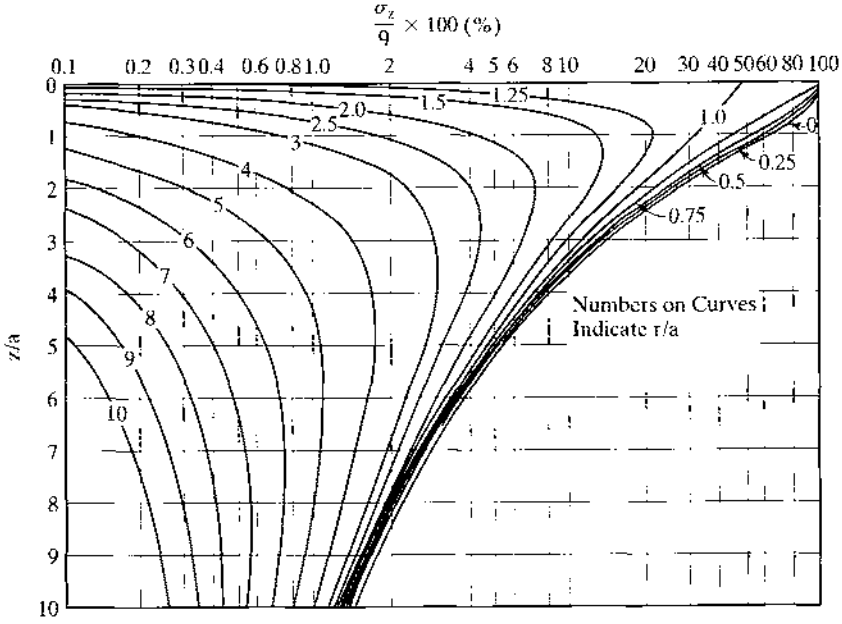

FIGURE 2.2

Vertical stresses due to circular loading. (After Foster and Ahlvin (1954).)

intensity q. Because Poisson ratio has a relatively small effect on stresses and deflections, Foster and Ahlvin assumed the half-space to be incompressible with a Poisson ratio of 0.5, so only one set of charts is needed instead of one for each Poisson ratio. This work was later refined by Ahlvin and Ulery (1962) who presented a series of

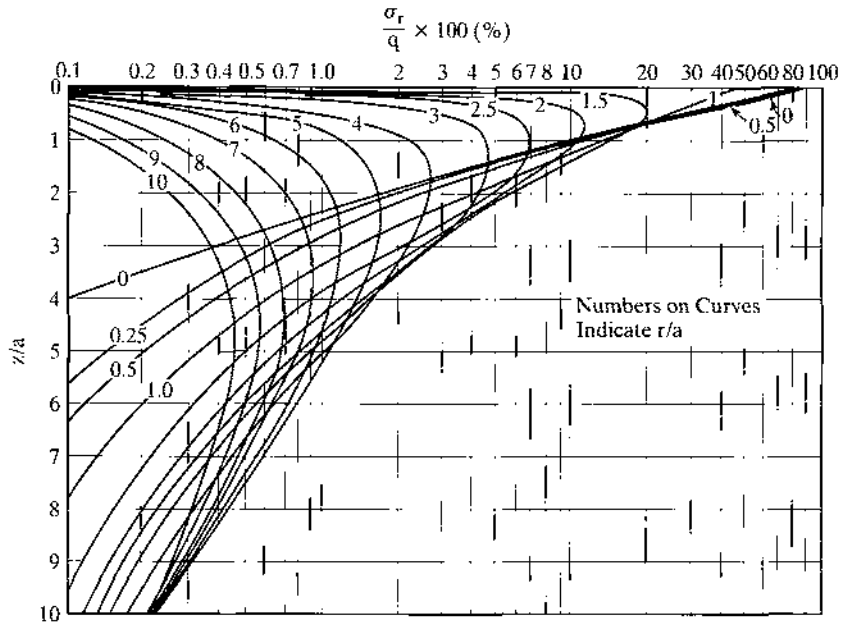

FIGURE 2.3

Radial stresses due to circular loading. (After Foster and Ahlvin, (1954).)

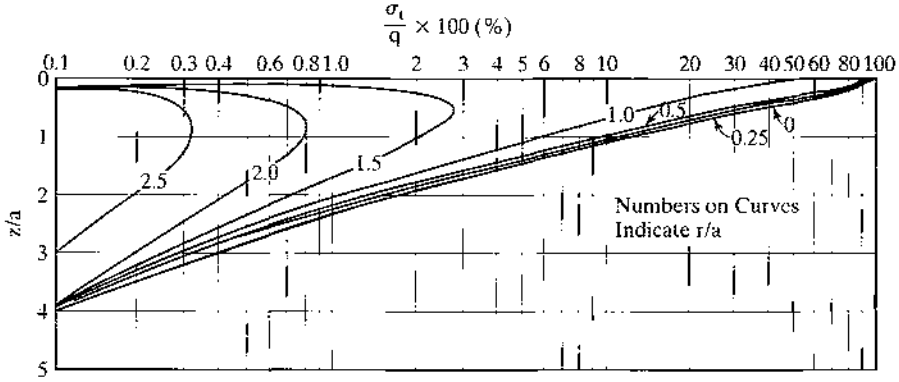

FIGURE 2.4

Tangential stresses due to circular loading. (After Foster and Ahlvin (1954).)

equations and tables so that the stresses, strains, and deflections for any given Poisson ratio can be computed. These equations and tables are not presented here because the solutions can be easily obtained from KENLAYER by assuming the homogeneous half-space to be a two-layer system, one of any thickness, but having the same elastic modulus and Poisson ratio for both layers.

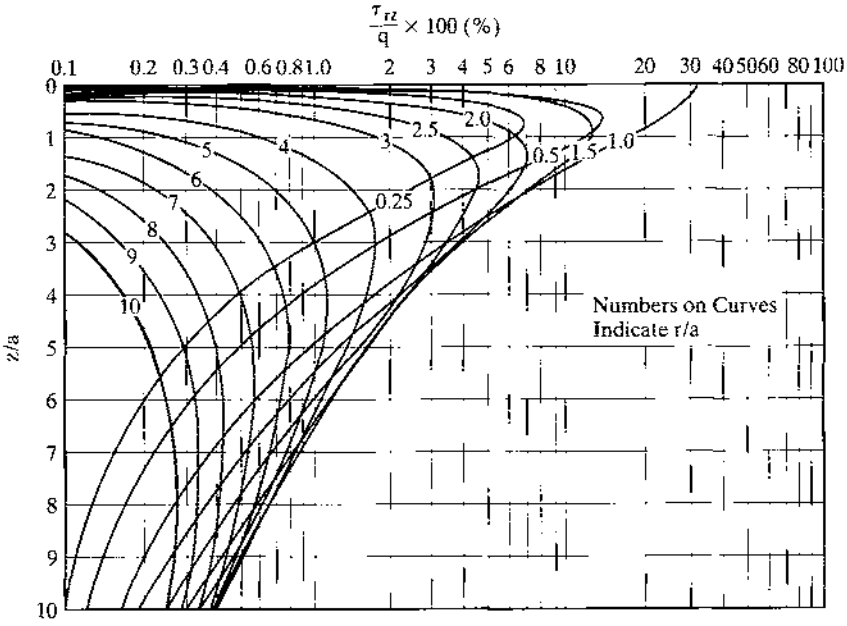

FIGURE 2.5

Shear stresses due to circular loading. (After Foster and Ahlvin (1954).)

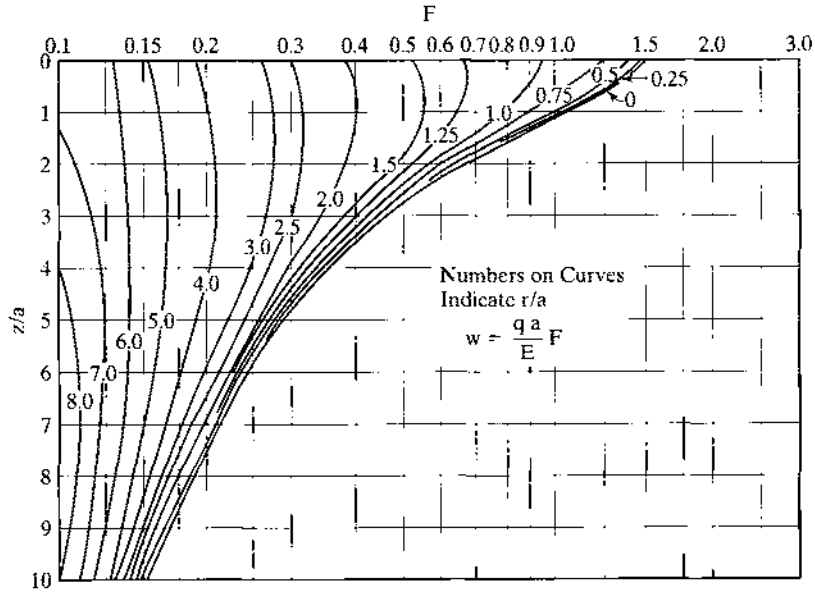

FIGURE 2.6

Vertical deflections due to circular loading. (After Foster and Ahlvin (1954).)

After the stresses are obtained from the charts, the strains can be obtained from

$$\epsilon_z = \frac{1}{E}[\sigma_z - v(\sigma_r + \sigma_t)] \tag{2.1a}$$

$$\epsilon_r = \frac{1}{E}[\sigma_r - v(\sigma_t + \sigma_z)] \tag{2.1b}$$

$$\epsilon_t = \frac{1}{E}[\sigma_t - v(\sigma_z + \sigma_r)] \tag{2.1c}$$

If the contact area consists of two circles, the stresses and strains can be computed by superposition.

Example 2.1:

Figure 2.7 shows a homogeneous half-space subjected to two circular loads, each 10 in. (254 mm) in diameter and spaced at 20 in. (508 mm) on centers. The pressure on the circular area is 50 psi (345 kPa). The half-space has elastic modulus 10,000 psi (69 MPa) and Poisson ratio 0.5. Determine the vertical stress, strain, and deflection at point A, which is located 10 in. (254 mm) below the center of one circle.

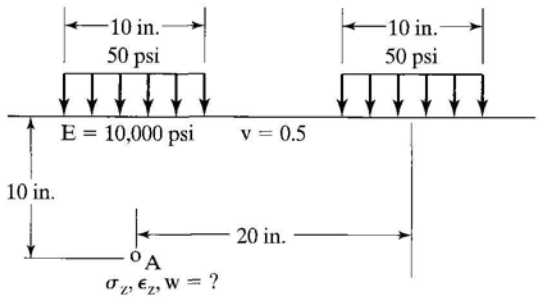

FIGURE 2.7
Example 2.1 (1 in. = 25.4 mm, psi = 6.9 kPa).

Solution: Given $a = 5$ in. (127 mm), $q = 50$ psi (345 kPa), and $z = 10$ in. (254 mm), from Figures 2.2, 2.3, and 2.4, the stresses at point A due to the left load with $r/a = 0$ and $z/a = 10/5 = 2$ are $\sigma_z = 0.28 \times 50 = 14.0$ psi (96.6 kPa) and $\sigma_r = \sigma_t = 0.016 \times 50 = 0.8$ psi (5.5 kPa); and those due to the right load with $r/a = 20/5 = 4$ and $z/a = 2$ are $\sigma_z = 0.0076 \times 50 = 0.38$ *psi (2.6 kPa)*, $\sigma_r = 0.026 \times 50 = 1.3$ psi (9.0 kPa), and $\sigma_t = 0$. By superposition, $\sigma_z = 14.0 + 0.38 = 14.38$ psi (99.2 kPa), $\sigma_r = 0.8 + 1.3 = 2.10$ psi (14.5 kPa), and $\sigma_t = 0.8$ psi (5.5 kPa). From Eq. 2.1*a*, $\epsilon_z = [14.38 - 0.5(2.10 + 0.8)]/10{,}000 = 0.00129$. From Figure 2.6, the deflection factor at point A due to the left load is 0.68 and that due to the right load is 0.21. The total deflection $w = (0.68 + 0.21) \times 50 \times 5/10{,}000 = 0.022$ in. (0.56 mm). The final answer is $\sigma_z = 14.38$ psi (99.2 kPa), $\epsilon_z = 0.00129$, and $w = 0.022$ in. (0.56 mm). The results obtained from KENLAYER are $\sigma_z = 14.6$ psi (100.7 kPa), $\epsilon_z = 0.00132$, and $w = 0.0218$ in. (0.554 mm), which check closely with those from the charts.

In applying Boussinesq's solutions, it is usually assumed that the pavement above the subgrade has no deformation, so the deflection on the pavement surface is equal to that on the top of the subgrade. In the above example, if the pavement thickness is 10 in. (254 mm) and point A is located on the surface of the subgrade, the deflection on the pavement surface is 0.022 in. (0.56 mm).

2.1.2 Solutions at Axis of Symmetry

When the load is applied over a single circular loaded area, the most critical stress, strain, and deflection occur under the center of the circular area on the axis of symmetry, where $\tau_{rz} = 0$ and $\sigma_r = \sigma_t$, so σ_z and σ_r are the principal stresses.

Flexible Plate The load applied from tire to pavement is similar to a flexible plate with a radius a and a uniform pressure q. The stresses beneath the center of the plate can be determined from

$$\sigma_z = q\left[1 - \frac{z^3}{(a^2 + z^2)^{1.5}}\right] \tag{2.2}$$

$$\sigma_r = \frac{q}{2}\left[1 + 2v - \frac{2(1 + v)z}{(a^2 + z^2)^{0.5}} + \frac{z^3}{(a^2 + z^2)^{1.5}}\right] \tag{2.3}$$

Note that σ_z is independent of E and v, and σ_r is independent of E. From Eq. 2.1,

$$\epsilon_z = \frac{(1 + v)q}{E}\left[1 - 2v + \frac{2vz}{(a^2 + z^2)^{0.5}} - \frac{z^3}{(a^2 + z^2)^{1.5}}\right] \tag{2.4}$$

$$\epsilon_r = \frac{(1 + v)q}{2E}\left[1 - 2v - \frac{2(1 - v)z}{(a^2 + z^2)^{0.5}} + \frac{z^3}{(a^2 + z^2)^{1.5}}\right] \tag{2.5}$$

The vertical deflection w can be determined from

$$w = \frac{(1 + v)qa}{E}\left\{\frac{a}{(a^2 + z^2)^{0.5}} + \frac{1 - 2v}{a}\left[(a^2 + z^2)^{0.5} - z\right]\right\} \tag{2.6}$$

When $v = 0.5$, Eq. 2.6 can be simplified to

$$w = \frac{3qa^2}{2E(a^2 + z^2)^{0.5}} \tag{2.7}$$

On the surface of the half-space, $z = 0$; from Eq. 2.6,

$$w_0 = \frac{2(1 - v^2)qa}{E} \tag{2.8}$$

Example 2.2:

Same as Example 2.1, except that only the left loaded area exists and the Poisson ratio is 0.3, as shown in Figure 2.8. Determine the stresses, strains, and deflection at point A.

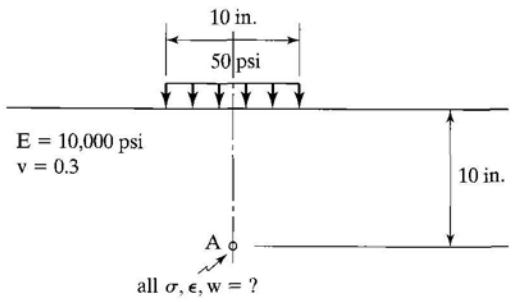

FIGURE 2.8

Example 2.2 (1 in. = 25.4 mm, 1 psi = 6.9 kPa).

Solution: Given $a = 5$ in. (127 mm), $q = 50$ psi (345 kPa), and $z = 10$ in. (254 mm), from Eq. 2.2, $\sigma_z = 50[1 - 1000/(25 + 100)^{1.5}] = 14.2$ psi (98.0 kPa). With $v = 0.3$, from Eq. 2.3, $\sigma_r = 25[1 + 0.6 - 2.6 \times 10/(125)^{0.5} + 1000/(125)^{1.5}] = -0.25$ psi (-1.7 kPa). The negative sign indicates tension, which is in contrast to a compressive stress of 0.8 psi (5.5 kPa) when $v = 0.5$. From Eq. 2.4, $\epsilon_z = 1.3 \times 50/10{,}000\,[1 - 0.6 + 0.6 \times 10/(125)^{0.5} - 1000/(125)^{1.5}] = 0.00144$. From Eq. 2.5, $\epsilon_r = 1.3 \times 50/20{,}000\,[1 - 0.6 - 1.4 \times 10/(125)^{0.5} + 1000/(125)^{1.5}] = -0.00044$. From Eq. 2.6, $w = 1.3 \times 50 \times 5/10{,}000\,\{5/(125)^{0.5} + 0.4/5[(125)^{0.5} - 10]\} = 0.0176$ in. (0.447 mm). The results obtained from KENLAYER are $\sigma_z = 14.2$ psi (98.0 kPa), $\sigma_r = -0.249$ psi (-1.72 kPa), $\epsilon_z = 0.00144$, $\epsilon_r = -0.000444$, and $w = 0.0176$ in. (0.447 mm), which are nearly the same as those derived from the formulas.

Rigid Plate All the above analyses are based on the assumption that the load is applied on a flexible plate, such as a rubber tire. If the load is applied on a rigid plate, such as that used in a plate loading test, the deflection is the same at all points on the plate, but the pressure distribution under the plate is not uniform. The differences between a flexible and a rigid plate are shown in Figure 2.9.

The pressure distribution under a rigid plate can be expressed as (Ullidtz, 1987)

$$q(r) = \frac{qa}{2(a^2 - r^2)^{0.5}} \tag{2.9}$$

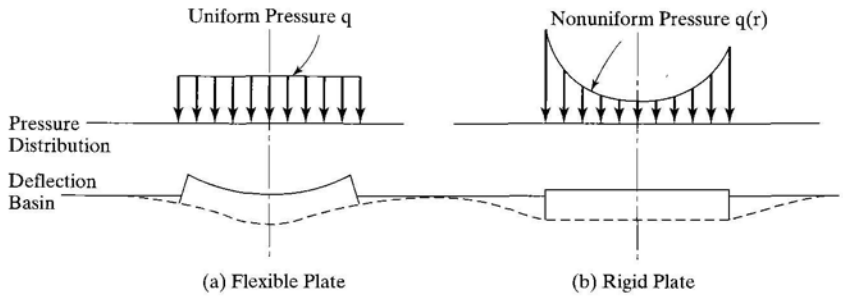

FIGURE 2.9

Differences between flexible and rigid plates.

in which r is the distance from center to the point where pressure is to be determined and q is the average pressure, which is equal to the total load divided by the area. The smallest pressure is at the center and equal to one-half of the average pressure. The pressure at the edge of the plate is infinity. By integrating the point load over the area, it can be shown that the deflection of the plate is

$$w_0 = \frac{\pi(1 - v^2)qa}{2E} \tag{2.10}$$

A comparison of Eq. 2.10 with Eq. 2.8 indicates that the surface deflection under a rigid plate is only 79% of that under the center of a uniformly distributed load. This is reasonable because the pressure under the rigid plate is smaller near the center of the loaded area but greater near the edge. The pressure near the center has a greater effect on the surface deflection at the center. Although Eqs. 2.8 and 2.10 are based on a homogeneous half-space, the same factor, 0.79, can be applied if the plates are placed on a layer system, as indicated by Yoder and Witczak (1975).

Example 2.3:

A plate loading test using a plate of 12-in. (305-mm) diameter was performed on the surface of the subgrade, as shown in Figure 2.10. A total load of 8000 lb (35.6 kN) was applied to the plate, and a deflection of 0.1 in. (2.54 mm) was measured. Assuming that the subgrade has Poisson ratio 0.4, determine the elastic modulus of the subgrade.

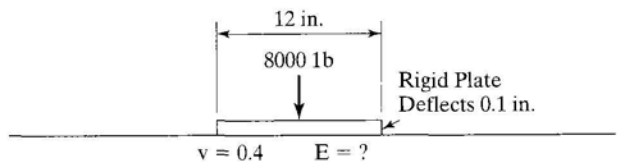

FIGURE 2.10
Example 2.3 (1 = 25.4 mm, 1 lb = 4.45 N).

Solution: The average pressure on the plate is $q = 8000/(36\pi) = 70.74$ psi (488 kPa). From Eq. 2.10, $E = \pi(1 - 0.16) \times 70.74 \times 6/(2 \times 0.1) = 5600$ psi (38.6 MPa).

2.1.3 Nonlinear Mass

Boussinesq's solutions are based on the assumption that the material that constitutes the half-space is linear elastic. It is well known that subgrade soils are not elastic and undergo permanent deformation under stationary loads. However, under the repeated application of moving traffic loads, most of the deformations are recoverable and can be considered elastic. It is therefore possible to select a reasonable elastic modulus commensurate with the speed of moving loads. Linearity implies the applicability of the superposition principle, so the elastic constant must not vary with the state of stresses. In other words, the axial deformation of a linear elastic material under an axial stress should be independent of the confining pressure. This is evidently not true for

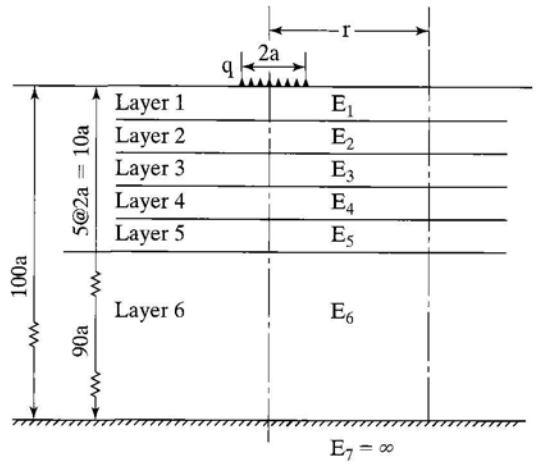

FIGURE 2.11
Division of half-space into a seven-layer system.

soils, because their axial deformation depends strongly on the magnitude of confining pressures. Consequently, the effect of nonlinearity on Boussinesq's solution is of practical interest.

Iterative Method To show the effect of nonlinearity of granular materials on vertical stresses and deflections, Huang (1968a) divided the half-space into seven layers, as shown in Figure 2.11, and applied Burmister's layered theory to determine the stresses at the midheight of each layer. Note that the lowest layer is a rigid base with a very large elastic modulus.

After the stresses are obtained, the elastic modulus of each layer is determined from

$$E = E_0(1 + \beta\theta) \tag{2.11}$$

in which θ is the stress invariant, or the sum of three normal stresses; E is the elastic modulus under the given stress invariant; E_0 is the initial elastic modulus, or the modulus when the stress invariant is zero; and β is a soil constant indicating the increase in elastic modulus per unit increase in stress invariant. Note that the stress invariant should include both the effects of the applied load and the geostatic stresses; it can be expressed as

$$\theta = \sigma_z + \sigma_r + \sigma_t + \gamma z(1 + 2K_0) \tag{2.12}$$

in which σ_z, σ_r, and σ_t are the vertical, radial, and tangential stresses due to loading; γ is the unit weight of soil; z is the distance below ground surface at which the stress invariant is computed; and K_0 is the coefficient of earth pressure at rest. The problem can be solved by a method of successive approximations. First, an elastic modulus is assumed for each layer and the stresses are obtained from the layered theory. Given

the stresses thus obtained, a new set of moduli is determined from Eq. 2.11 and a new set of stresses is then computed. The process is repeated until the moduli between two consecutive iterations converge to a specified tolerance.

In applying the layered theory for nonlinear analysis, a question immediately arises: Which radial distance r should be used to determine the stresses and the moduli? Huang (1968a) showed that the vertical stresses are not affected significantly by whether the stresses at $r = 0$ or $r = \infty$ are used to determine the elastic modulus, but the vertical displacements are tremendously affected. He later used the finite-element method and found that the nonlinear behavior of soils has a large effect on vertical and radial displacements, an intermediate effect on radial and tangential stresses, and a very small effect on vertical and shear stresses (Huang, 1969a). Depending on the depth of the point in question, the vertical stresses based on nonlinear theory may be greater or smaller than those based on linear theory and, at a certain depth, both theories could yield the same stresses. This may explain why Boussinesq's solutions for vertical stress based on linear theory have been applied to soils with varying degrees of success, even though soils themselves are basically nonlinear.

Approximate Method One approximate method to analyze a nonlinear half-space is to divide it into a number of layers and determine the stresses at the midheight of each layer by Boussinesq's equations based on linear theory. From the stresses thus obtained, the elastic modulus E for each layer is determined from Eq. 2.11. The deformation of each layer, which is the difference in deflection between the top and bottom of each layer based on the given E, can then be obtained. Starting from the rigid base, or a depth far from the surface where the vertical displacement can be assumed zero, the deformations are added to obtain the deflections at various depths. The assumption of Boussinesq's stress distribution was used by Vesic and Domaschuk (1964) to predict the shape of deflection basins on highway pavements, and satisfactory agreements were reported.

It should be noted that Eq. 2.11 is one of the many constitutive equations for sands. Uzan (1985), Pezo *et al.* (1992), and Pezo (1993) assumed that the modulus of granular materials depended not only on the stress invariant, θ, but also on the deviator stress, which is the difference between major and minor principal stresses. This concept has been used in the 2002 Design Guide, as presented in Appendix F. Other constitutive relationships for sands or clays can also be used, as discussed in Section 3.1.4.

Example 2.4:

A circular load having radius 6 in. (152 mm) and contact pressure 80 psi (552 kPa) is applied on the surface of a subgrade. The subgrade soil is a sand with the relationship between the elastic modulus and the stress invariant shown in Figure 2.12*a*. The soil has Poisson ratio 0.3, the mass unit weight is 110 pcf (17.3 kN/m^3), and the coefficient of earth pressure at rest is 0.5. The soil is divided into six layers, as shown in Figure 2.12*b*. Determine the vertical surface displacement at the axis of symmetry.

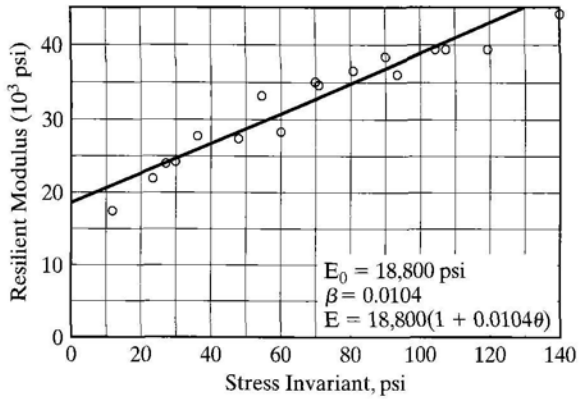

(a) Resilient Modulus

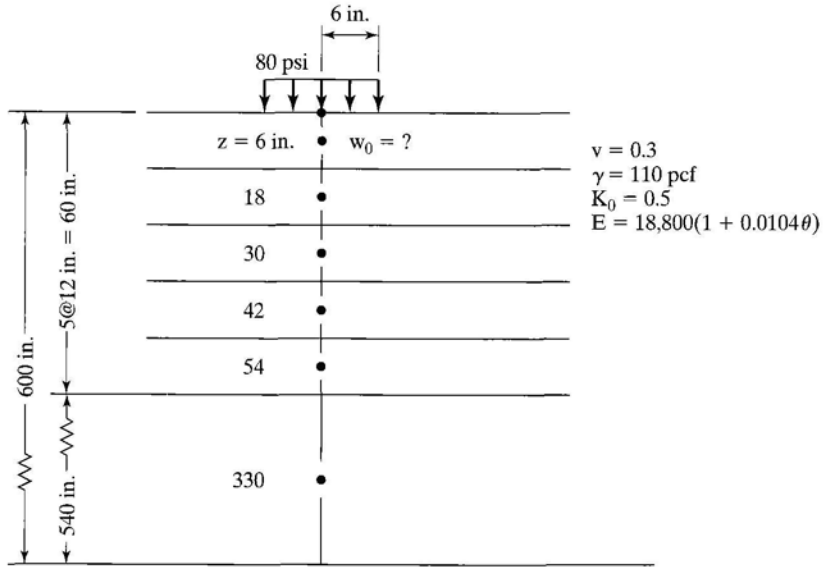

(b) Layer Subdivision

FIGURE 2.12

Example 2.4 (1 in. = 25.4 mm, 1 psi = 6.9 kPa, 1 pcf = 157.1 N/m^3).

Solution: At the midheight of layer 1, $z = 6$ in. (152 mm). From Eq. 2.2, $\sigma_z = 80[1 - 216/(36 + 36)^{1.5}] = 51.7$ psi (357 kPa). From Eq. 2.3, $\sigma_r = \sigma_t = 40\,[1 + 2 \times 0.3 - 2.6 \times 6/(72)^{0.5} + 216/(72)^{1.5}] = 4.60$ psi (31.7 kPa). From Eq. 2.12, $\theta = 51.7 + 4.6 + 4.6 + 110 \times 6\,(1 + 2 \times 0.5)/(12)^3 = 61.7$ psi (426 kPa). From Eq. 2.11 with $E_0 = 18{,}800$ psi (130 MPa) and $\beta = 0.0104$, as shown in Figure 2.12*a*, $E = 18{,}800\,(1 + 0.0104 \times 61.7) = 30{,}900$ psi (213 MPa). From Eq. 2.6, the deflection at top, when $z = 0$, $w = 1.3 \times 80 \times 6\,(1 + 1 - 0.6)/30{,}900 = 0.0283$ in. (0.719 mm), and the deflection at bottom, when $z = 12$ in. (305 mm), $w = 1.3 \times 80 \times 6\,\{6/(36 + 144)^{0.5} + 0.4[(180)^{0.5} - 12]/6\}/30{,}900 = 0.0109$ in. (0.277 mm). The deformation for layer 1 is $0.0283 - 0.0109 = 0.0174$ in. (0.442 mm). The deformations for other layers can be determined similarly, and the results are tabulated in Table 2.1.

TABLE 2.1 Computation of Deformation for Each Layer

Layer no.	Thickness (in.)	z at mid-height (in.)	σ_z (psi)	σ_r (psi)	θ (psi)		E (psi)	wE (lb/in.)	Deformation (in.)
					Loading	Geostatic			
								873.6	
1	12	6	51.72	4.60	60.92	0.76	30,860		0.0174
								338.0	
2	12	18	11.69	−0.51	10.67	2.29	21,330		0.0073
								182.1	
3	12	30	4.57	−0.27	4.03	3.82	20,330		0.0029
								123.2	
4	12	42	2.39	−0.15	2.09	5.35	20,250		0.0015
								92.9	
5	12	54	1.46	−0.09	1.28	6.88	20,400		0.0009
								74.5	
6	540	330	0.04	0.00	0.04	42.01	27,020		0.0025
								7.5	
							Total		0.0325

Note. 1 in. = 25.4 mm, 1 psi = 6.9 kPa, 1 lb/in. = 175 N/m.

To compute the deformation of each layer, the product of w and E at each layer interface is first determined from Eq. 2.6. The difference in wE between the two interfaces divided by E gives the deformation of the layer. The surface deflection is the sum of all layer deformations and equals to 0.0325 in. (0.826 mm). It is interesting to note that the stress invariant θ due to the applied load decreases with depth, while that due to geostatic stresses increases with depth. As a result, the elastic moduli for all layers, except layers 1 and 6, become nearly the same. Note also that more than 50% of the surface deflections are contributed by the deformation in the top 12 in. (305 mm).

The same problem was solved by KENLAYER after the incorporation of Eq. 2.11 into the program. The differences in stress distribution between Boussinesq and Burmister theory and the resulting moduli are shown in Table 2.2. It can be seen that the two solutions correspond well. The surface deflection based on layered theory

TABLE 2.2 Differences in Stresses and Moduli between Boussinesq and Burmister Solutions

z at midheight (in.)	Boussinesq			Burmister		
	σ_z (psi)	σ_r (psi)	E (psi)	σ_z (psi)	σ_r (psi)	E (psi)
6	51.72	4.60	30,860	50.46	4.50	30,580
18	11.69	−0.51	21,330	10.61	−0.65	21,070
30	4.57	−0.27	20,330	4.26	−0.27	20,280
42	2.39	−0.15	20,250	2.31	−0.11	20,260
54	1.46	−0.09	20,400	1.47	0.01	20,440
330	0.04	0.00	27,020	0.04	0.00	27,020

Note. 1 in. = 25.4 mm, 1 psi = 6.9 kPa.

is 0.0310 in. (0.787 mm), which also agrees with the 0.0325 in. (0.826 mm) from Boussinesq theory.

2.2 LAYERED SYSTEMS

Flexible pavements are layered systems with better materials on top and cannot be represented by a homogeneous mass, so the use of Burmister's layered theory is more appropriate. Burmister (1943) first developed solutions for a two-layer system and then extended them to a three-layer system (Burmister, 1945). With the advent of computers, the theory can be applied to a multilayer system with any number of layers (Huang, 1967, 1968a).

Figure 2.13 shows an n-layer system. The basic assumptions to be satisfied are:

1. Each layer is homogeneous, isotropic, and linearly elastic with an elastic modulus E and a Poisson ratio v.
2. The material is weightless and infinite in areal extent.
3. Each layer has a finite thickness h, except that the lowest layer is infinite in thickness.
4. A uniform pressure q is applied on the surface over a circular area of radius a.
5. Continuity conditions are satisfied at the layer interfaces, as indicated by the same vertical stress, shear stress, vertical displacement, and radial displacement. For frictionless interface, the continuity of shear stress and radial displacement is replaced by zero shear stress at each side of the interface.

In this section, only some of the solutions on two- and three-layer systems with bonded interfaces are presented. The theoretical development of multilayer systems is discussed in Appendix B.

2.2.1 Two-Layer Systems

The exact case of a two-layer system is the full-depth construction in which a thick layer of HMA is placed directly on the subgrade. If a pavement is composed of three

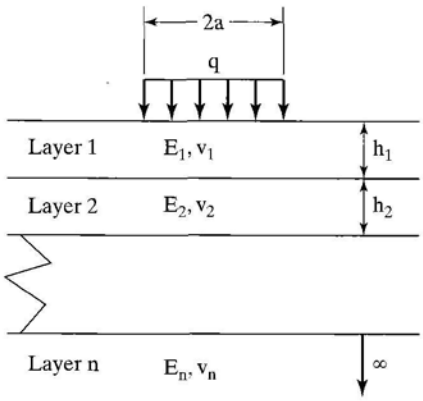

FIGURE 2.13
An n-layer system subjected to a circular load.

layers (e.g., an asphalt surface course, a granular base course, and a subgrade), it is necessary to combine the base course and the subgrade into a single layer for computing the stresses and strains in the asphalt layer or to combine the asphalt surface course and base course for computing the stresses and strains in the subgrade.

Vertical Stress The vertical stress on the top of subgrade is an important factor in pavement design. The function of a pavement is to reduce the vertical stress on the subgrade so that detrimental pavement deformations will not occur. The allowable vertical stress on a given subgrade depends on the strength or modulus of the subgrade. To combine the effect of stress and strength, the vertical compressive strain has been used most frequently as a design criterion. This simplification is valid for highway and airport pavements because the vertical strain is caused primarily by the vertical stress and the effect of horizontal stress is relatively small. As pointed out in Section 1.5.2, the design of railroad trackbeds should be based on vertical stress instead of vertical strain, because the large horizontal stress caused by the distribution of wheel loads through rails and ties over a large area makes the vertical strain a poor indicator of the vertical stress.

The stresses in a two-layer system depend on the modulus ratio E_1/E_2 and the thickness–radius ratio h_1/a. Figure 2.14 shows the effect of a pavement layer on the distribution of vertical stresses under the center of a circular loaded area. The chart is applicable to the case when the thickness h_1 of layer 1 is equal to the radius of contact area, or $h_1/a = 1$. As in all charts presented in this section, a Poisson ratio of 0.5 is assumed for all layers. It can be seen that the vertical stresses decrease significantly with the increase in modulus ratio. At the pavement–subgrade interface, the vertical stress is about 68% of the applied pressure if $E_1/E_2 = 1$, as indicated by Boussinesq's stress distribution, and reduces to about 8% of the applied pressure if $E_1/E_2 = 100$.

Figure 2.15 shows the effect of pavement thickness and modulus ratio on the vertical stress σ_c at the pavement–subgrade interface under the center of a circular loaded area. For a given applied pressure q, the vertical stress increases with the increase in contact radius and decreases with the increase in thickness. The reason that the ratio a/h_1 instead of h_1/a was used is for the purpose of preparing influence charts (Huang, 1969b) for two-layer elastic foundations.

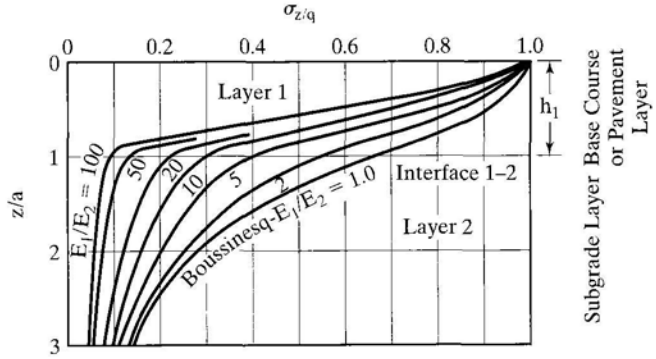

FIGURE 2.14

Vertical stress distribution in a two-layer system. (After Burmister (1958).)

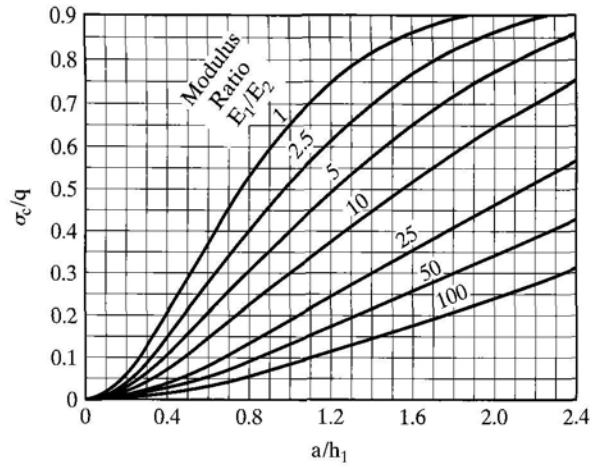

FIGURE 2.15

Vertical interface stresses for two-layer systems. (After Huang (1969b).)

Example 2.5:

A circular load having radius 6 in. (152 mm) and uniform pressure 80 psi (552 kPa) is applied on a two-layer system, as shown in Figure 2.16. The subgrade has elastic modulus 5000 psi (35 MPa) and can support a maximum vertical stress of 8 psi (55 kPa). If the HMA has elastic modulus 500,000 psi (3.45 GPa), what is the required thickness of a full-depth pavement? If a thin surface treatment is applied on a granular base with elastic modulus 25,000 psi (173 MPa), what is the thickness of base course required?

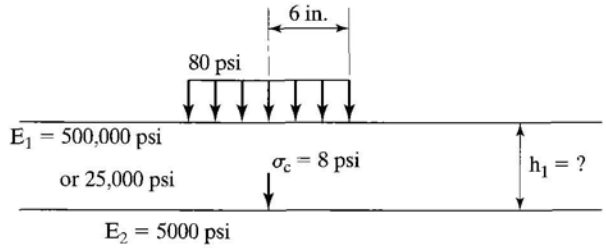

FIGURE 2.16

Example 2.5 (1 in. = 25.4 mm, 1 psi = 6.9 kPa).

Solution: Given $E_1/E_2 = 500{,}000/5000 = 100$ and $\sigma_c/q = 8/80 = 0.1$, from Figure 2.15, $a/h_1 = 1.15$, or $h_1 = 6/1.15 = 5.2$ in. (132 mm), which is the minimum thickness for full depth. Given $E_1/E_2 = 25{,}000/5000 = 5$ and $\sigma_c/q = 0.1$, from Figure 2.15, $a/h_1 = 0.4$, or $h_1 = 6/0.4 = 15$ in. (381 mm), which is the minimum thickness of granular base required.

In this example, an allowable vertical stress of 8 psi (55 kPa) is arbitrarily selected to show the effect of the modulus of the reinforced layer on the thickness required. The allowable vertical stress should depend on the number of load repetitions. Using the Shell design criterion and the AASHTO equation, Huang et al. (1984b) developed the relationship

$$N_d = 4.873 \times 10^{-5} \sigma_c^{-3.734} E_2^{3.583} \tag{2.13}$$

in which N_d is the allowable number of stress repetitions to limit permanent deformation, σ_c is the vertical compressive stress on the surface of the subgrade in psi, and E_2 is

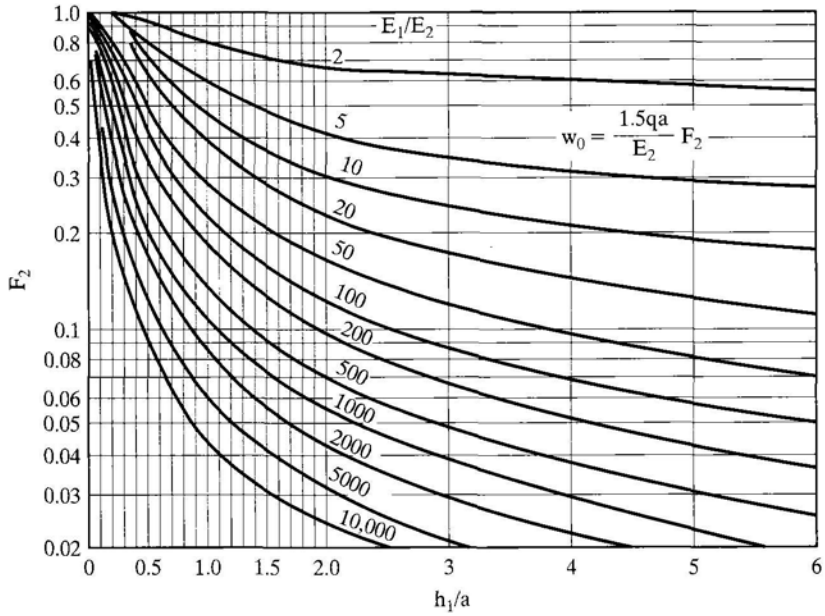

FIGURE 2.17

Vertical surface deflections for two-layer systems. (After Burmister (1943).)

the elastic modulus of the subgrade in psi. For a stress of 8 psi (5 kPa) and an elastic modulus of 5000 psi (35 MPa), the allowable number of repetitions is 3.7×10^5.

Vertical Surface Deflection Vertical surface deflections have been used as a criterion of pavement design. Figure 2.17 can be used to determine the surface deflections for two-layer systems. The deflection is expressed in terms of the deflection factor F_2 by

$$w_0 = \frac{1.5qa}{E_2} F_2 \tag{2.14}$$

The deflection factor is a function of E_1/E_2 and h_1/a. For a homogeneous half-space with $h_1/a = 0$, $F_2 = 1$, so Eq. 2.14 is identical to Eq. 2.8 when $v = 0.5$. If the load is applied by a rigid plate, then, from Eq 2.10,

$$w_0 = \frac{1.18qa}{E_2} F_2 \tag{2.15}$$

Example 2.6:

A total load of 20,000 lb (89 kN) was applied on the surface of a two-layer system through a rigid plate 12 in. (305 mm) in diameter, as shown in Figure 2.18. Layer 1 has a thickness of 8 in. (203 mm) and layer 2 has an elastic modulus of 6400 psi (44.2 MPa). Both layers are incompressible with a Poisson ratio of 0.5. If the deflection of the plate is 0.1 in. (2.54 mm), determine the elastic modulus of layer 1.

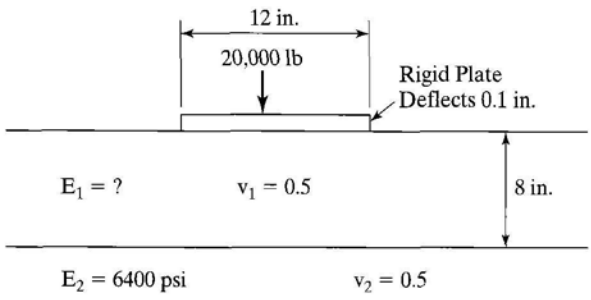

FIGURE 2.18

Example 2.6 (in. = 25.4 mm, 1 psi = 6.9 kPa, 1 lb = 4.45 N).

Solution: The average pressure on the plate is $q = 20{,}000/(36\pi) = 176.8$ psi (1.22 MPa). From Eq. 2.15, $F_2 = 0.1 \times 6400/(1.18 \times 176.8 \times 6) = 0.511$. Given $h_1/a = 8/6 = 1.333$, from Figure 2.17, $E_1/E_2 = 5$, or $E_1 = 5 \times 6400 = 32{,}000$ psi (221 MPa).

Vertical Interface Deflection The vertical interface deflection has also been used as a design criterion. Figure 2.19 can be used to determine the vertical interface deflection in a two-layer system (Huang, 1969c). The deflection is expressed in terms of the deflection factor F by

$$w = \frac{qa}{E_2}F \tag{2.16}$$

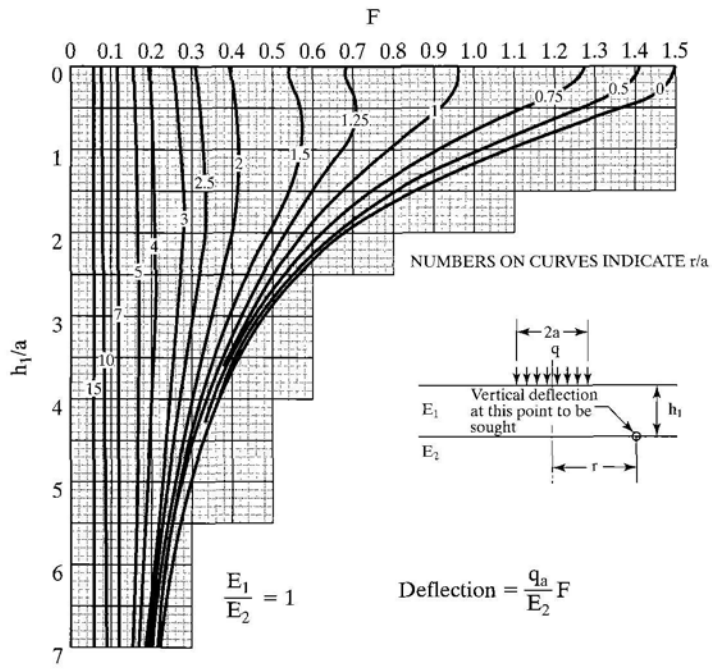

FIGURE 2.19

Vertical interface deflections for two-layer systems. (After Huang (1969c).)

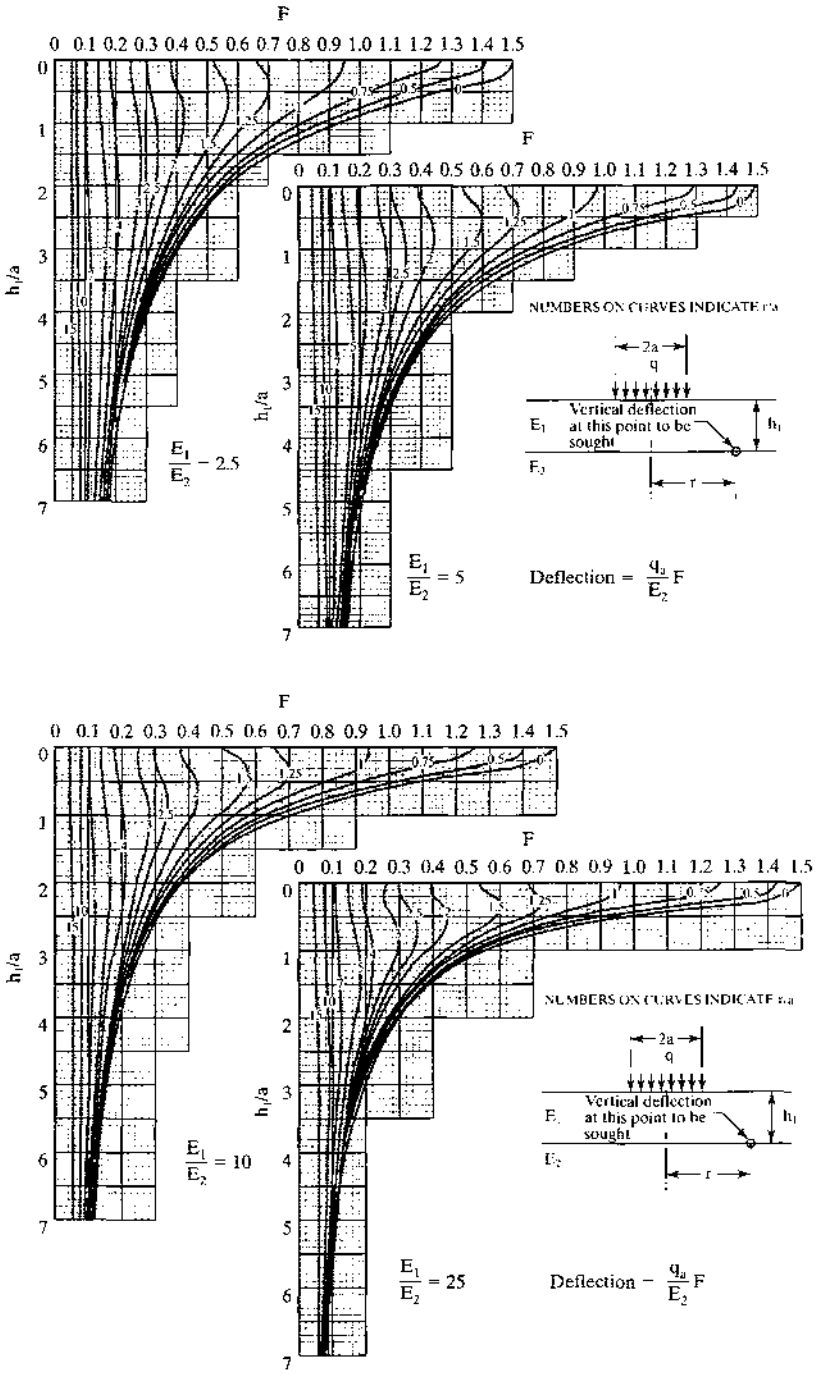

FIGURE 2.19 (Continued)

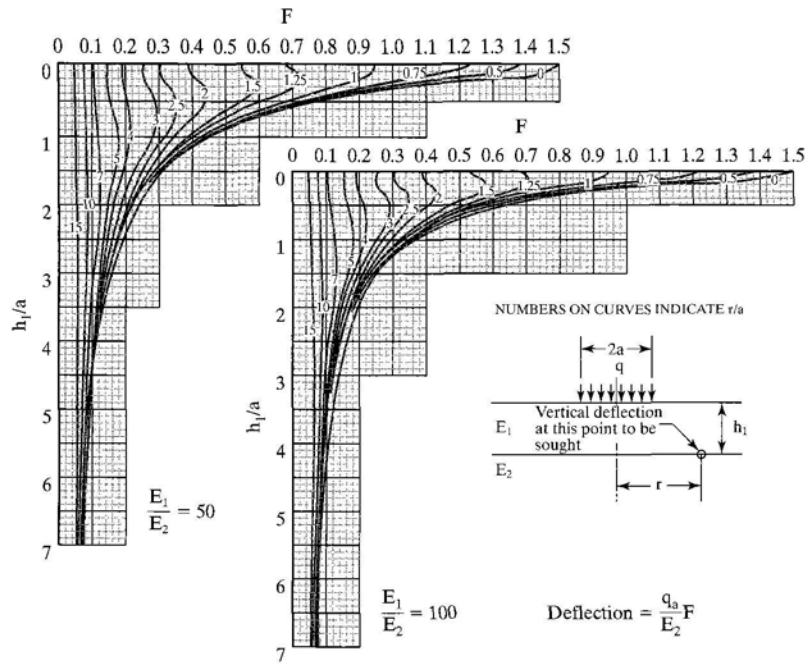

FIGURE 2.19 (Continued)

Note that F in Eq. 2.16 is different from F_2 in Eq. 2.14 by the factor 1.5. The deflection factor is a function of E_1/E_2, h_1/a, and r/a, where r is the radial distance from the center of loaded area. Seven sets of charts for the modulus ratios 1, 2.5, 5, 10, 25, 50, and 100, are shown; the deflection for any intermediate modulus ratio can be obtained by interpolation. The case of $E_1/E_2 = 1$ is Boussinesq's solution.

Example 2.7:

Figure 2.20 shows a set of dual tires, each having contact radius 4.52 in. (115 mm) and contact pressure 70 psi (483 kPa). The center-to-center spacing of the dual is 13.5 in. (343 mm). Layer 1 has thickness 6 in. (152 mm) and elastic modulus 100,000 psi (690 MPa); layer 2 has elastic modulus 10,000 psi (69 MPa). Determine the vertical deflection at point A, which is on the interface beneath the center of one loaded area.

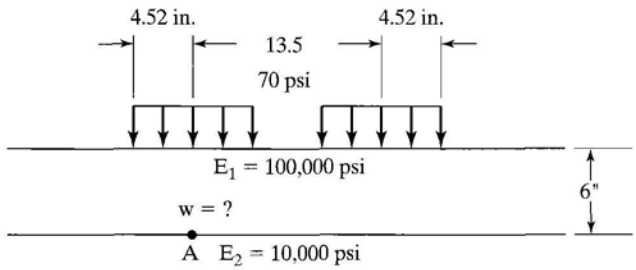

FIGURE 2.20

Example 2.7 (1 in. = 25.4 mm, 1 psi = 6.9 kPa).

Solution: Given $E_1/E_2 = 100{,}000/10{,}000 = 10$ and $h_1/a = 6/4.52 = 1.33$, from Figure 2.19, the deflection factor at point A due to the left load with $r/a = 0$ is 0.56 and that due to the right load with $r/a = 13.5/4.52 = 2.99$ is 0.28. By superposition, $F = 0.56 + 0.28 = 0.84$. From Eq. 2.16, $w = 70 \times 4.52/10{,}000 \times 0.84 = 0.027$ in. (0.69 mm). The interface deflection obtained from KENLAYER is 0.0281 in. (0.714 mm), which checks well with the chart solution.

It should be pointed out that the maximum interface deflection under dual tires might not occur at point A. To determine the maximum interface deflection, it is necessary to compute the deflection at several points, say one under the center of one tire, one at the center between two tires, and the other under the edge of one tire, and find out which is maximum.

Critical Tensile Strain The tensile strains at the bottom of asphalt layer have been used as a design criterion to prevent fatigue cracking. Two types of principal strains could be considered. One is the overall principal strain based on all six components of normal and shear stresses. The other, which is more popular and was used in KENLAYER, is the horizontal principal strain based on the horizontal normal and shear stresses only. The overall principal strain is slightly greater than the horizontal principal strain, so the use of overall principal strain is on the safe side.

Huang (1973a) developed charts for determining the critical tensile strain at the bottom of layer 1 for a two-layer system. The critical tensile strain is the overall strain and can be determined from

$$e = \frac{q}{E_1} F_e \tag{2.17}$$

in which e is the critical tensile strain and F_e is the strain factor, which can be determined from the charts.

Single Wheel Figure 2.21 presents the strain factor for a two-layer system under a circular loaded area. In most cases, the critical tensile strain occurs under the center

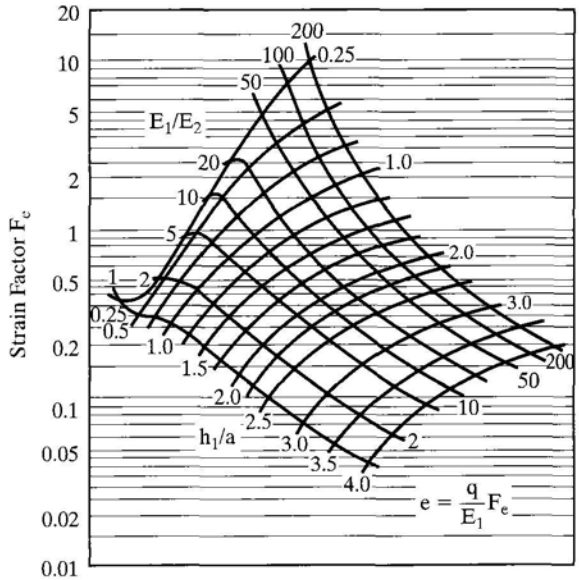

FIGURE 2.21

Strain factor for single wheel. (After Huang (1973a).)

of the loaded area, where the shear stress is zero. However, when both h_1/a and E_1/E_2 are small, the critical tensile strain occurs at some distance from the center, as the predominant effect of the shear stress. Under such situations, the principal tensile strains at the radial distances 0, $0.5a$, a, and $1.5a$ from the center were computed, and the critical value was obtained and plotted in Figure 2.21.

Example 2.8:

Figure 2.22 shows a full-depth asphalt pavement 8 in. (203 mm) thick subjected to a single-wheel load of 9000 lb (40 kN) having contact pressure 67.7 psi (467 kPa). If the elastic modulus of the asphalt layer is 150,000 psi (1.04 GPa) and that of the subgrade is 15,000 psi (104 MPa), determine the critical tensile strain in the asphalt layer.

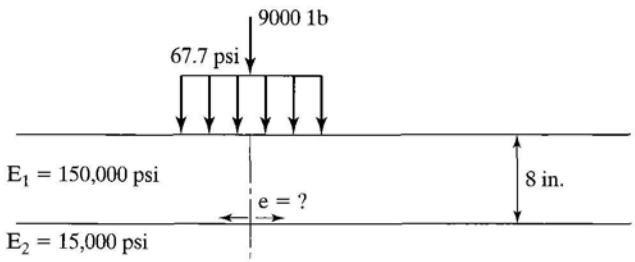

FIGURE 2.22

Example 2.8 (1 in. = 25.4 mm, 1 psi = 6.9 kPa, 1 lb = 4.45 N).

Solution: Given $a = \sqrt{9000/(\pi \times 67.7)} = 6.5$ in. (165 mm), $h_1/a = 8/6.5 = 1.23$, and $E_1/E_2 = 150{,}000/15{,}000 = 10$, from Figure 2.21, $F_e = 0.72$. From Eq. 2.17, the critical tensile strain $e = 67.7 \times 0.72/150{,}000 = 3.25 \times 10^{-4}$, which checks well with the 3.36×10^{-4} obtained by KENLAYER.

It is interesting to note that the bonded interface makes the horizontal tensile strain at the bottom of layer 1 equal to the horizontal tensile strain at the top of layer 2. If layer 2 is incompressible and the critical tensile strain occurs on the axis of symmetry, then the vertical compressive strain is equal to twice the horizontal strain, as shown by Eq. 2.21 (as is discussed later). Therefore, Figure 2.21 can be used to determine the vertical compressive strain on the surface of the subgrade as well.

Dual Wheels Because the strain factor for dual wheels with a contact radius a and a dual spacing S_d depends on S_d/a in addition to E_1/E_2 and h_1/a, the most direct method is to present charts similar to Figure 2.21, one for each value of S_d/a. However, this approach requires a series of charts, and the interpolation could be quite time-consuming. To avoid these difficulties, a unique method was developed that requires only one chart, as shown in Figure 2.23.

In this method, the dual wheels are replaced by a single wheel with the same contact radius a, so that Figure 2.21 can still be used. Because the strain factor for dual wheels is generally greater than that for a single wheel, a conversion factor C, which is the ratio between dual- and single-wheel strain factors, must be determined. Multiplication of

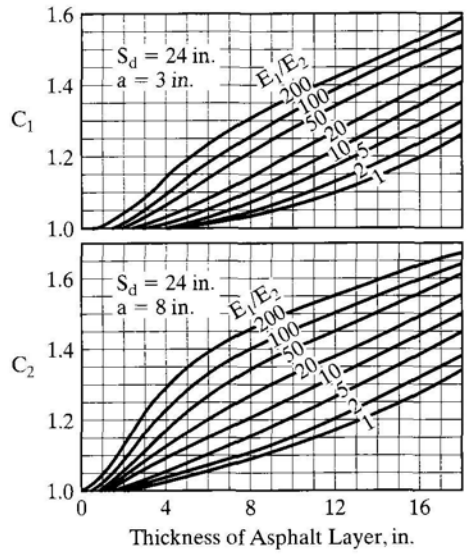

FIGURE 2.23

Conversion factor for dual wheel (1 in. = 25.4 mm). (After Huang (1973a).)

the conversion factor by the strain factor obtained from Figure 2.21 will yield the strain factor for dual wheels.

The two-layer theory indicates that the strain factor for dual wheels depends on h_1/a, S_d/a, and E_1/E_2. As long as the ratios h_1/a and S_d/a remain the same, the strain factor will be the same, no matter how large or small the contact radius a may be. Consider a set of dual wheels with $S_d = 24$ in. (610 mm) and $a = 3$ in. (76 mm). The strain factors for various values of h_1 and E_1/E_2 were calculated and the conversion factors were obtained and plotted as a set of curves on the upper part of Figure 2.23. Another set of curves based on the same S_d but with $a = 8$ in. (203 mm) is plotted at the bottom. It can be seen that, for the same dual spacing, the larger the contact radius, the larger the conversion factor. However, the change in conversion factor due to the change in contact radius is not very large, so a straight-line interpolation should give a fairly accurate conversion factor for any other contact radii. Although Figure 2.23 is based on $S_d = 24$ in. (610 mm), it can be applied to any given S_d by simply changing a and h_1 in proportion to the change in S_d, so that the ratios h_1/a and S_d/a remain the same. The procedure can be summarized as follows:

1. From the given S_d, h_1, and a, determine the modified radius a' and the modified thickness h_1':

$$a' = \frac{24}{S_d} a \tag{2.18a}$$

$$h_1' = \frac{24}{S_d} h_1 \tag{2.18b}$$

2. Using h_1' as the pavement thickness, find conversion factors C_1 and C_2 from Figure 2.23.

3. Determine the conversion factor for a' by a straight-line interpolation between 3 and 8 in. (76 and 203 mm), or

$$C = C_1 + 0.2 \times (a' - 3) \times (C_2 - C_1) \tag{2.19}$$

Example 2.9:

For the same pavement as in Example 2.8, if the 9000-lb (40-kN) load is applied over a set of dual tires with a center-to-center spacing of 11.5 in. (292 mm) and a contact pressure of 67.7 psi (467 kPa), as shown in Figure 2.24, determine the critical tensile strain in the asphalt layer.

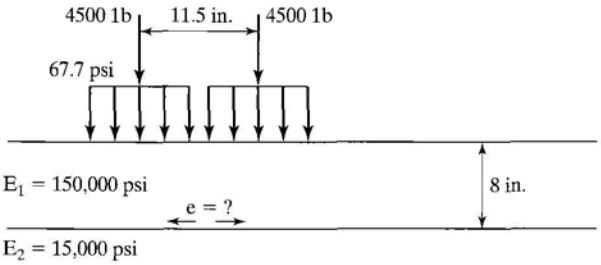

FIGURE 2.24

Example 2.9 (1 in. = 25.4 mm, 1 psi = 6.9 kPa, 1 lb = 4.45 N).

Solution: Given $a = \sqrt{4500/(\pi \times 67.7)} = 4.6$ in. (117 mm), $S_d = 11.5$ in. (292 mm), and $h_1 = 8$ in. (203 mm), from Eq. 2.18, $a' = 24 \times 4.6/11.5 = 9.6$ in. (244 mm) and $h_1' = 24 \times 8/11.5 = 16.7$ in. (424 mm). With $E_1/E_2 = 10$ and an asphalt layer thickness of 16.7 in. (424 mm), from Figure 2.23, $C_1 = 1.35$ and $C_2 = 1.46$. From Eq. 2.19, $C = 1.35 + 0.2\,(9.6 - 3)(1.46 - 1.35) = 1.50$. From Figure 2.21, the strain factor for a single wheel = 0.47 and that for dual wheels = $1.50 \times 0.47 = 0.705$, so the critical tensile strain $e = 67.7 \times 0.705/150{,}000 = 3.18 \times 10^{-4}$, which checks closely with the 3.21×10^{-4} obtained by KENLAYER.

By comparing the results of Examples 2.8 and 2.9, it can be seen that, in this particular case (when the asphalt layer is thick and the dual spacing is small), a load applied on a set of dual tires yields a critical strain that is not very different from that on a single wheel. However, this is not true when thin asphalt layers or large dual spacings are involved.

Huang (1972) also presented a simple chart for determining directly the maximum tensile strain in a two-layer system subjected to a set of dual tires spaced at a distance of $3a$ on center. A series of charts relating tensile strains to curvatures was also developed, so that the tensile strain under a design dual-wheel load can be evaluated in the field by simply measuring the curvature on the surface (Huang, 1971).

Dual-Tandem Wheels Charts similar to Figure 2.23 with dual spacing S_d of 24 in. (610 mm) and tandem spacings S_t of 24 in. (610 mm), 48 in. (1220 mm), and 72 in. (1830 mm) were developed for determining the conversion factor due to dual-tandem wheels, as shown in Figures 2.25, 2.26, and 2.27. The use of these charts is similar to the use of Figure 2.23. Because the conversion factor for dual-tandem wheels depends on h_1/a, S_d/a, and S_t/a, and because the actual S_d may not be equal to 24 in. (610 mm), it is

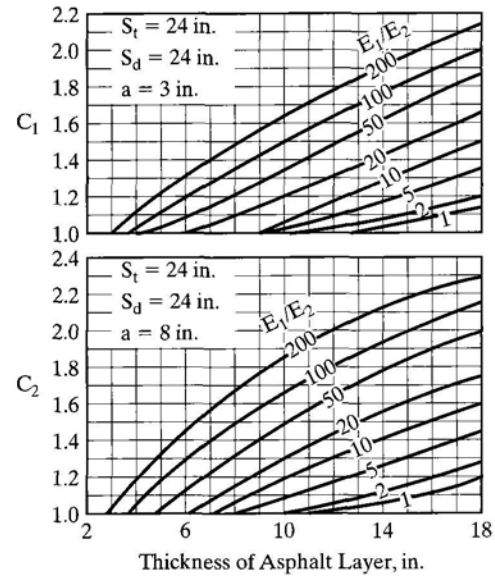

FIGURE 2.25

Conversion factor for dual-tandem wheels with 24-in. tandem spacing (1 in. = 25.4 mm). (After Huang (1973a).)

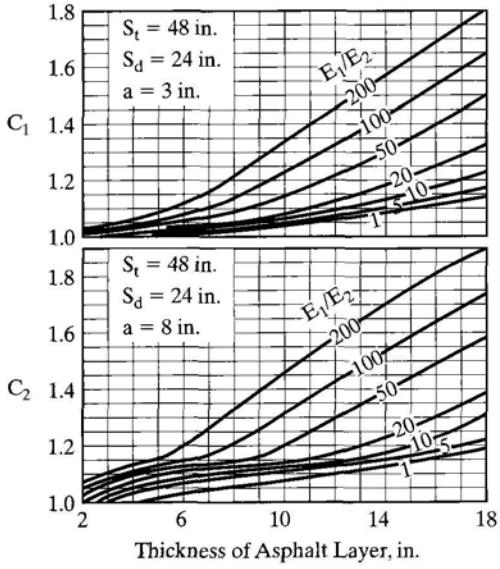

FIGURE 2.26

Conversion factor for dual-tandem wheels with 48-in. tandem spacing (1 in. = 25.4 mm). (After Huang (1973a).)

necessary to change S_d to 24 in. (610 mm) and then change the contact radius a proportionately according to Eq. 2.18*a*, thus keeping the ratio S_d/a unchanged.

The values of h_1 and S_t must also be changed accordingly to keep h_1/a and S_t/a unchanged. Therefore, the original problem is changed to a new problem with S_d = 24 in. (610 mm) and a new S_t. The conversion factor for S_t = 24, 48, and 72 in. (0.61, 1.22, and 1.83 m) can be obtained from the charts; that for other values of S_t can be determined by interpolation.

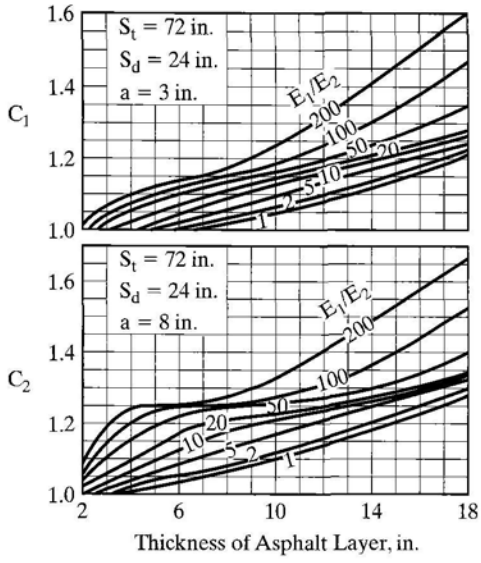

FIGURE 2.27

Conversion factor for dual-tandem wheels with 72-in. tandem spacing (1 in. = 25.4 mm). (After Huang (1973a).)

If the new values of S_t are greater than 72 in. (1.83 m), Figure 2.23, based on dual wheels can be used for interpolation. In fact, Figure 2.23 is a special case of dual-tandem wheels when the tandem spacing approaches infinity. It was found that, when S_t = 120 in. (3.05 m) the conversion factor due to dual-tandem wheels does not differ significantly from that due to dual wheels alone, so Figure 2.23 can be considered to have a tandem spacing of 120 in. (3.05 m).

A comparison of Figure 2.23 with Figures 2.25 through 2.27 clearly indicates that, in many cases, the addition of tandem wheels reduces the conversion factor, thus decreasing the critical tensile strain. This is due to the compensative effect caused by the additional wheels. The interaction among these wheels is quite unpredictable, as indicated by the irregular shape of the curves in the lower part of Figures 2.26 and 2.27.

Example 2.10:

Same as example 2.9, except that an identical set of duals is added to form dual-tandem wheels having the tandem spacing 49 in. (1.25 m), as shown in Figure 2.28.

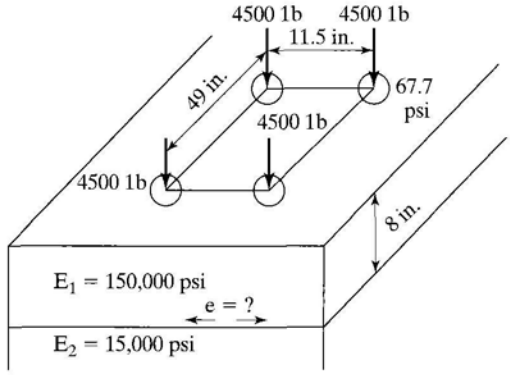

FIGURE 2.28

Example 2.10 (1 in. = 25.4 mm, 1 psi = 6.9 kPa, 1 lb = 4.45 N).

Solution: Given S_d = 11.5 in. (292 mm) and S_t = 49 in. (1.25 m), modified tandem spacing = 49 × 24/11.5 = 102.3 in. (2.60 m). Values of a' and h' are the same as in Example 2.8. When S_t = 72 in. (1.83 m), a' = 9.6 in. (244 mm), and h_1' = 16.7 in. (424 mm), from Figure 2.27, C = 1.23 + 0.2 (9.6 − 3)(1.30 − 1.23) = 1.32, which is smaller than the 1.5 for the dual wheels alone. With a conversion factor of 1.32 for S_t = 72 in. (1.83 m) and 1.50 for S_t = 120 in. (3.05 m), by straight-line interpolation, C = 1.32 + (1.50 − 1.32)(102.3 − 72)/(120 − 72) = 1.43. The strain factor due to dual-tandem wheels = 1.43 × 0.47 = 0.672. Critical tensile strain = 67.7 × 0.672/150,000 = 3.03 × 10^{-4}, which checks closely with the 3.05 × 10^{-4} obtained from KENLAYER.

2.2.2 Three-Layer Systems

Figure 2.29 shows a three-layer system and the stresses at the interfaces on the axis of symmetry. These stresses include vertical stress at interface 1, σ_{z1}, vertical stress at interface 2, σ_{z2}, radial stress at bottom of layer 1, σ_{r1}, radial stress at top of layer 2, σ'_{r1}, radial stress at bottom of layer 2, σ_{r2}, and radial stress at top of layer 3, σ'_{r2}. Note that, on the axis of symmetry, tangential and radial stresses are identical and the sheer stress is equal to 0.

When the Poisson ratio is 0.5, we have, from Eq. 2.1,

$$\epsilon_z = \frac{1}{E}(\sigma_z - \sigma_r) \tag{2.20a}$$

$$\epsilon_r = \frac{1}{2E}(\sigma_r - \sigma_z) \tag{2.20b}$$

Equation 2.20 indicates that the radial strain equals one-half of the vertical strain and is opposite in sign, or

$$\epsilon_z = -2\epsilon_r \tag{2.21}$$

Equation 2.21 can be visualized physically from the fact that, when a material is incompressible and has the Poisson ratio 0.5, the horizontal strain is equal to one-half of the vertical strain and the sum of ϵ_z, ϵ_r, and ϵ_t must be equal to 0.

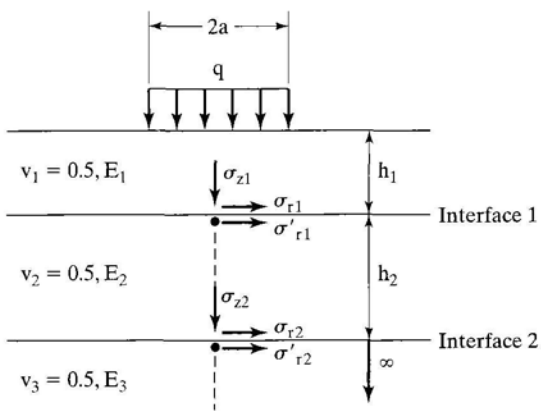

FIGURE 2.29

Stresses at interfaces of a three-layer system.

Jones' Tables The stresses in a three-layer system depend on the ratios k_1, k_2, A, and H, defined as

$$k_1 = \frac{E_1}{E_2} \qquad k_2 = \frac{E_2}{E_3} \tag{2.22a}$$

$$A = \frac{a}{h_2} \qquad H = \frac{h_1}{h_2} \tag{2.22b}$$

Jones (1962) presented a series of tables for determining σ_{z1}, $\sigma_{z1} - \sigma_{r1}$, σ_{z2}, and $\sigma_{z2} - \sigma_{r2}$. His tables also include values of $\sigma_{z1} - \sigma'_{r1}$ at the top of layer 2 and $\sigma_{z2} - \sigma'_{r2}$ at the top of layer 3, but these tabulations are actually not necessary because they can be easily determined from those at the bottom of layers 1 and 2. The continuity of horizontal displacement at the interface implies that the radial strains at the bottom of one layer are equal to that at the top of the next layer, or, from Eq. 2.20*b*,

$$\sigma_{z1} - \sigma'_{r1} = \frac{\sigma_{z1} - \sigma_{r1}}{k_1} \tag{2.23a}$$

$$\sigma_{z2} - \sigma'_{r2} = \frac{\sigma_{z2} - \sigma_{r2}}{k_2} \tag{2.23b}$$

The tables presented by Jones consist of four values of k_1 and k_2 (0.2, 2, 20, and 200), so solutions for intermediate values of k_1 and k_2 can be obtained by interpolation. In view of the fact that solutions for three-layer systems can be easily obtained by KENLAYER and the interpolation from the tables is impractical and requires a large amount of time and effort, only the more realistic cases (k_1 = 2, 20, and 200, and k_2 = 2 and 20) are presented, to conserve space.

Table 2.3 presents the stress factors for three-layer systems. The sign convention is positive in compression and negative in tension. Four sets of stress factors,—ZZ1, ZZ2, ZZ1 − RR1, and ZZ2 − RR2—are shown. The product of the contact pressure and the stress factors gives the stresses:

$$\sigma_{z1} = q\,(\text{ZZ1}) \tag{2.24a}$$

$$\sigma_{z2} = q\,(\text{ZZ2}) \tag{2.24b}$$

$$\sigma_{z1} - \sigma_{r1} = q\,(\text{ZZ1} - \text{RR1}) \tag{2.24c}$$

$$\sigma_{z2} - \sigma_{r2} = q\,(\text{ZZ2} - \text{RR2}) \tag{2.24d}$$

Example 2.11:

Given the three-layer system shown in Figure 2.30 with a = 4.8 in. (122 mm), q = 120 psi (828 kPa), h_1 = 6 in. (152 mm), h_2 = 6 in. (203 mm), E_1 = 400,000 psi (2.8 GPa), E_2 = 20,000 psi (138 MPa), and E_3 = 10,000 psi (69 MPa), determine all the stresses and strains at the two interfaces on the axis of symmetry.

TABLE 2.3 Stress Factors for Three-Layer Systems

			$k_1 = 2$				$k_1 = 20$				$k_1 = 200$			
H	k_2	A	ZZ1	ZZ2	(ZZ1 − RR1)	(ZZ2 − RR2)	ZZ1	ZZ2	(ZZ1 − RR1)	(ZZ2 − RR2)	ZZ1	ZZ2	(ZZ1 − RR1)	(ZZ2 − RR2)
		0.1	0.42950	0.00896	0.70622	0.01716	0.14529	0.00810	1.81178	0.01542	0.03481	0.00549	3.02259	0.00969
		0.2	0.78424	0.03493	0.97956	0.06647	0.38799	0.03170	3.76886	0.06003	0.11491	0.02167	8.02452	0.03812
	2	0.4	0.98044	0.12667	0.70970	0.23531	0.78651	0.11650	5.16717	0.21640	0.33218	0.08229	17.64175	0.14286
		0.8	0.99434	0.36932	0.22319	0.63003	1.02218	0.34941	3.43631	0.60493	0.72695	0.27307	27.27701	0.45208
		1.6	0.99364	0.72113	−0.19982	0.97707	0.99060	0.69014	1.15211	0.97146	1.00203	0.63916	23.38638	0.90861
		3.2	0.99922	0.96148	−0.28916	0.84030	0.99893	0.93487	−0.06894	0.88358	1.00828	0.92560	11.87014	0.91469
0.125														
		0.1	0.43022	0.00228	0.69332	0.03467	0.14447	0.00182	1.80664	0.02985	0.03336	0.00128	3.17763	0.01980
		0.2	0.78414	0.00899	0.92086	0.13541	0.38469	0.00716	3.74573	0.11697	0.10928	0.00509	8.66097	0.07827
	20	0.4	0.97493	0.03392	0.46583	0.49523	0.77394	0.02710	5.05489	0.43263	0.31094	0.01972	20.12259	0.29887
		0.8	0.97806	0.11350	−0.66535	1.49612	0.98610	0.09061	2.92533	1.33736	0.65934	0.07045	36.29943	1.01694
		1.6	0.96921	0.31263	−2.82859	3.28512	0.93712	0.24528	−1.27093	2.99215	0.87931	0.20963	49.40857	2.64313
		3.2	0.98591	0.68433	−5.27906	5.05952	0.96330	0.55490	−7.35384	5.06489	0.93309	0.49938	57.84369	4.89895
		0.1	0.15524	0.00710	0.28362	0.01353	0.04381	0.00530	0.63215	0.00962	0.00909	0.00259	0.96553	0.00407
		0.2	0.42809	0.02783	0.70225	0.05278	0.14282	0.02091	1.83766	0.03781	0.03269	0.01027	3.10763	0.01611
	2	0.4	0.77939	0.10306	0.96634	0.19178	0.37882	0.07933	3.86779	0.14159	0.10684	0.04000	8.37852	0.06221
		0.8	0.96703	0.31771	0.66885	0.55211	0.75904	0.26278	5.50796	0.44710	0.30477	0.14513	18.95534	0.21860
		1.6	0.98156	0.66753	0.17331	0.95080	0.98743	0.61673	4.24281	0.90115	0.66786	0.42940	31.18909	0.58553
		3.2	0.99840	0.93798	−0.05691	0.89390	1.00064	0.91258	1.97494	0.93254	0.98447	0.84545	28.98500	0.89191
0.25														
		0.1	0.15436	0.00179	0.25780	0.02728	0.04236	0.00123	0.65003	0.01930	0.00776	0.00065	1.08738	0.00861
		0.2	0.42462	0.00706	0.67115	0.10710	0.13708	0.00488	1.90693	0.07623	0.02741	0.00257	3.59448	0.03421
	20	0.4	0.76647	0.02697	0.84462	0.39919	0.35716	0.01888	4.13976	0.29072	0.08634	0.01014	10.30923	0.13365
		0.8	0.92757	0.09285	0.21951	1.26565	0.68947	0.06741	6.48948	0.98565	0.23137	0.03844	26.41442	0.49135
		1.6	0.91393	0.26454	−1.22411	2.94860	0.85490	0.20115	6.95639	2.55231	0.46835	0.13148	57.46409	1.53833
		3.2	0.95243	0.60754	−3.04320	4.89878	0.90325	0.48647	6.05854	4.76234	0.71083	0.37342	99.29034	3.60964
		0.1	0.04330	0.00465	0.08250	0.00878	0.01122	0.00259	0.17997	0.00440	0.00215	0.00094	0.26620	0.00128
		0.2	0.15325	0.01836	0.28318	0.03454	0.04172	0.01028	0.64779	0.01744	0.00826	0.00373	0.98772	0.00509
	2	0.4	0.42077	0.06974	0.70119	0.12954	0.13480	0.03998	1.89817	0.06722	0.02946	0.01474	3.19580	0.01996
		0.8	0.75683	0.23256	0.96681	0.41187	0.35175	0.14419	4.09592	0.23476	0.09508	0.05622	8.71973	0.07434
		1.6	0.93447	0.56298	0.70726	0.85930	0.70221	0.42106	6.22002	0.62046	0.27135	0.19358	20.15765	0.23838
		3.2	0.98801	0.88655	0.33878	0.96353	0.97420	0.82256	5.41828	0.93831	0.62399	0.52912	34.25229	0.54931
0.5														
		0.1	0.04193	0.00117	0.08044	0.01778	0.00990	0.00063	0.19872	0.00911	0.00149	0.00023	0.31847	0.00257
		0.2	0.14808	0.00464	0.27574	0.07027	0.03648	0.00251	0.72264	0.03620	0.00564	0.00094	1.19598	0.01025
	20	0.4	0.40086	0.01799	0.67174	0.26817	0.11448	0.00988	2.19520	0.14116	0.01911	0.00372	1.02732	0.04047
		0.8	0.69098	0.06476	0.86191	0.91168	0.27934	0.03731	5.24726	0.51585	0.05574	0.01453	12.00885	0.15452
		1.6	0.79338	0.19803	0.39588	2.38377	0.50790	0.12654	10.30212	1.59341	0.13946	0.05399	32.77028	0.53836
		3.2	0.85940	0.49238	−0.41078	4.47022	0.70903	0.35807	16.38520	3.69109	0.30247	0.18091	77.62943	1.56409

		0.1	0.01083	0.00241	0.02179	0.00453	0.00263	0.00100	0.04751	0.00160	0.00049	0.00029	0.06883	0.00035
		0.2	0.04176	0.00958	0.08337	0.01797	0.01029	0.00347	0.18481	0.00637	0.00195	0.00116	0.26966	0.00138
	2	0.4	0.14665	0.03724	0.28491	0.06934	0.03810	0.01565	0.66727	0.02498	0.00746	0.00460	1.00131	0.00545
		0.8	0.39942	0.13401	0.71341	0.24250	0.12173	0.05938	1.97428	0.09268	0.02647	0.01797	3.24971	0.02092
		1.6	0.71032	0.38690	1.02680	0.63631	0.31575	0.20098	4.37407	0.29253	0.08556	0.06671	8.92442	0.07335
		3.2	0.92112	0.75805	0.90482	0.97509	0.66041	0.53398	6.97695	0.65446	0.25186	0.22047	20.83387	0.21288
1														
		0.1	0.00963	0.00061	0.02249	0.00920	0.00193	0.00024	0.05737	0.00322	0.00027	0.00007	0.08469	0.00062
		0.2	0.03697	0.00241	0.08618	0.03654	0.00751	0.00098	0.22418	0.01283	0.00104	0.00028	0.33312	0.00248
	20	0.4	0.12805	0.00950	0.29640	0.14241	0.02713	0.00387	0.82430	0.05063	0.00384	0.00110	1.25495	0.00985
		0.8	0.33263	0.03578	0.76292	0.51815	0.08027	0.01507	2.59672	0.19267	0.01236	0.00436	4.26100	0.03825
		1.6	0.52721	0.12007	1.25168	1.56503	0.17961	0.05549	6.77014	0.66326	0.03379	0.01683	12.91809	0.13989
		3.2	0.65530	0.33669	1.70723	3.51128	0.34355	0.18344	15.23252	1.88634	0.08859	0.06167	36.04291	0.45544
		0.1	0.00250	0.00100	0.00555	0.00188	0.00059	0.00033	0.01219	0.00051	0.00011	0.00008	0.01737	0.00009
		0.2	0.00991	0.00397	0.02199	0.00750	0.00235	0.00130	0.04843	0.00203	0.00045	0.00033	0.06913	0.00036
	2	0.4	0.03832	0.01569	0.08465	0.02950	0.00922	0.00518	0.18857	0.00803	0.00179	0.00131	0.27103	0.00142
		0.8	0.13516	0.05974	0.29365	0.11080	0.03412	0.02023	0.68382	0.03093	0.00685	0.00520	1.00808	0.00553
		1.6	0.36644	0.20145	0.75087	0.35515	0.10918	0.07444	2.04134	0.10864	0.02441	0.02003	3.27590	0.02043
		3.2	0.67384	0.51156	1.17294	0.77434	0.29183	0.23852	4.60426	0.30709	0.08061	0.07248	9.02195	0.06638
2														
		0.1	0.00181	0.00025	0.00652	0.00378	0.00033	0.00008	0.01568	0.00094	0.00005	0.00002	0.02160	0.00014
		0.2	0.00716	0.00099	0.02586	0.01507	0.00130	0.00031	0.06236	0.00374	0.00018	0.00007	0.08604	0.00058
	20	0.4	0.02746	0.00394	0.10017	0.05958	0.00503	0.00123	0.24425	0.01486	0.00071	0.00030	0.33866	0.00229
		0.8	0.09396	0.01535	0.35641	0.22795	0.01782	0.00485	0.90594	0.05789	0.00261	0.00119	1.27835	0.00901
		1.6	0.23065	0.05599	1.00785	0.78347	0.05012	0.01862	2.91994	0.21190	0.00819	0.00467	4.35311	0.03390
		3.2	0.37001	0.17843	2.16033	2.13215	0.11331	0.06728	7.95104	0.67732	0.02341	0.01784	13.26873	0.11666
		0.1	0.00057	0.00034	0.00147	0.00065	0.00013	0.00010	0.00312	0.00015	0.00003	0.00002	0.00437	0.00002
		0.2	0.00228	0.00137	0.00587	0.00260	0.00054	0.00039	0.01245	0.00029	0.00011	0.00009	0.01746	0.00009
	2	0.4	0.00905	0.00544	0.02324	0.01032	0.00214	0.00154	0.04944	0.00235	0.00042	0.00036	0.06947	0.00036
		0.8	0.03500	0.02135	0.08957	0.04031	0.00837	0.00610	0.19247	0.00924	0.00168	0.00142	0.27221	0.00144
		1.6	0.12354	0.07972	0.31215	0.14735	0.03109	0.02358	0.69749	0.03488	0.00646	0.00560	1.01140	0.00553
		3.2	0.34121	0.25441	0.81908	0.43632	0.10140	0.08444	2.09049	0.11553	0.02332	0.02126	3.28913	0.01951
4														
		0.1	0.00030	0.00008	0.00201	0.00128	0.00005	0.00002	0.00413	0.00025	0.00001	0.00000	0.00545	0.00003
		0.2	0.00119	0.00034	0.00803	0.00510	0.00021	0.00009	0.01651	0.00099	0.00003	0.00002	0.02178	0.00014
	20	0.4	0.00469	0.00134	0.03191	0.02032	0.00083	0.00035	0.06569	0.00396	0.00013	0.00008	0.08673	0.00054
		0.8	0.01790	0.00532	0.12427	0.07991	0.00321	0.00138	0.25739	0.01565	0.00050	0.00031	0.34131	0.00215
		1.6	0.06045	0.02049	0.45100	0.29991	0.01130	0.00542	0.95622	0.05993	0.00186	0.00124	1.28773	0.00833
		3.2	0.14979	0.07294	1.36427	0.97701	0.03258	0.02061	3.10980	0.20906	0.00612	0.00483	4.38974	0.03010

Source. After Jones (1962).

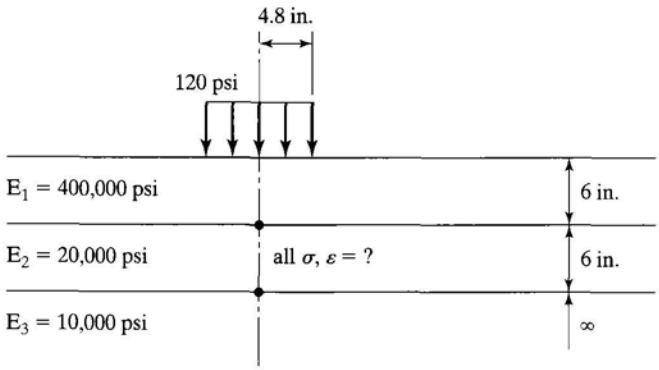

FIGURE 2.30

Example 2.11 (1 in. = 25.4 mm, 1 psi = 6.9 kPa).

Solution: Given $k_1 = 400{,}000/20{,}000 = 20$, $k_2 = 20{,}000/10{,}000 = 2$, $A = 4.8/6 = 0.8$, and $H = 6/6 = 1.0$, from Table 2.3, ZZ1 = 0.12173, ZZ2 = 0.05938, ZZ1 − RR1 = 1.97428, and ZZ2 − RR2 = 0.09268. From Eq. 2.24, $\sigma_{z1} = 120 \times 0.12173 = 14.61$ psi (101 kPa), $\sigma_{z2} = 120 \times 0.05938 = 7.12$ psi (49.1 kPa), $\sigma_{z1} - \sigma_{r1} = 120 \times 1.97428 = 236.91$ psi (1.63 MPa), and $\sigma_{z2} - \sigma_{r2} = 120 \times 0.09268 = 11.12$ psi (76.7 kPa). From Eq. 2.23, $\sigma_{z1} - \sigma'_{r1} = 236.91/20 = 11.85$ psi (81.8 kPa) and $\sigma_{z2} - \sigma'_{r2} = 11.12/2 = 5.56$ psi (38.4 kPa). At bottom of layer 1: $\sigma_{r1} = 14.61 - 236.91 = -222.3$ psi (−1.53 MPa), from Eq. 2.20, $\epsilon_z = 236.91/400{,}000 = 5.92 \times 10^{-4}$ and $\epsilon_r = -2.96 \times 10^{-4}$. At top of layer 2: $\sigma'_{r1} = 14.61 - 11.85 = 2.76$ psi (19.0 kPa), $\epsilon_z = 11.85/20{,}000 = 5.92 \times 10^{-4}$, and $\sigma_r = -2.96 \times 10^{-4}$. At bottom of layer 2: $\sigma_{r2} = 7.12 - 11.12 = -4.0$ psi (−28 kPa), $\epsilon_z = 11.12/20{,}000 = 5.56 \times 10^{-4}$, and $\epsilon_r = -2.78 \times 10^{-4}$. At top of layer 3: $\sigma'_{r2} = 7.12 - 5.56 = 1.56$ psi (10.8 kPa), $\epsilon_z = 5.56/10{,}000 = 5.56 \times 10^{-4}$ and $\epsilon_r = -2.78 \times 10^{-4}$.

In the foregoing example, the parameters k_1, k_2, A, and H are exactly the same as those shown in the table, so no interpolation is needed. Because each interpolation requires three points, the interpolation of only one parameter requires at least three times the effort. If all four parameters are different from those in the table, the total effort required will be $3 \times 3 \times 3 \times 3$, or 81 times.

Peattie's Charts Peattie (1962) plotted Jones' table in graphical forms. Figure 2.31 shows one set of charts for radial strain factors, (RR1 − ZZ1)/2, at the bottom of layer 1. As indicated by Eq. 2.20*b*, the radial strain can be determined from

$$\epsilon_r = \frac{q}{E}\left(\frac{\text{RR1} - \text{ZZ1}}{2}\right) \tag{2.25}$$

The radial strains at the bottom of layer 1 should be in tension. Although the solutions obtained from the charts are not as accurate as those from the table, the chart has the advantage that interpolation for A and H can be easily done. However, interpolation for k_1 and k_2 is still cumbersome.

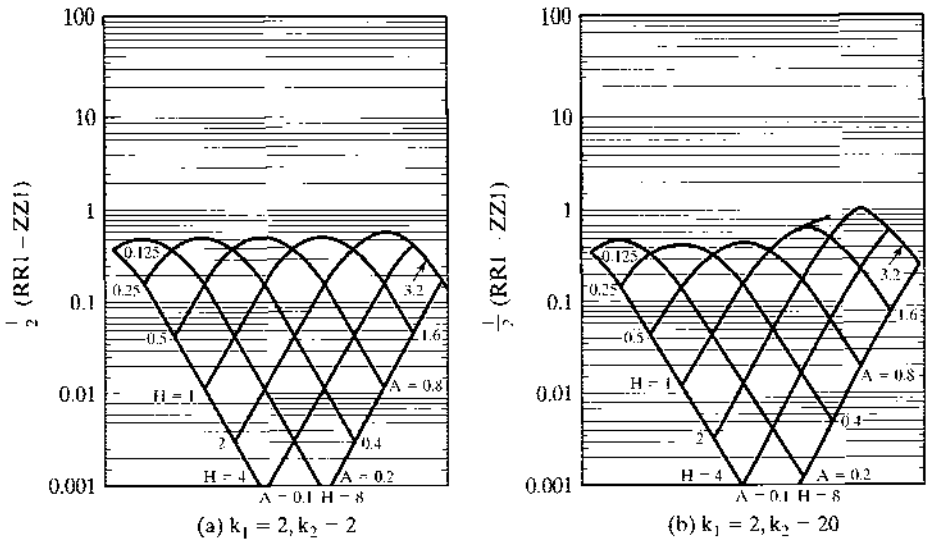

FIGURE 2.31

Charts for horizontal strain factors at bottom of layer 1. (After Peattie (1962).)

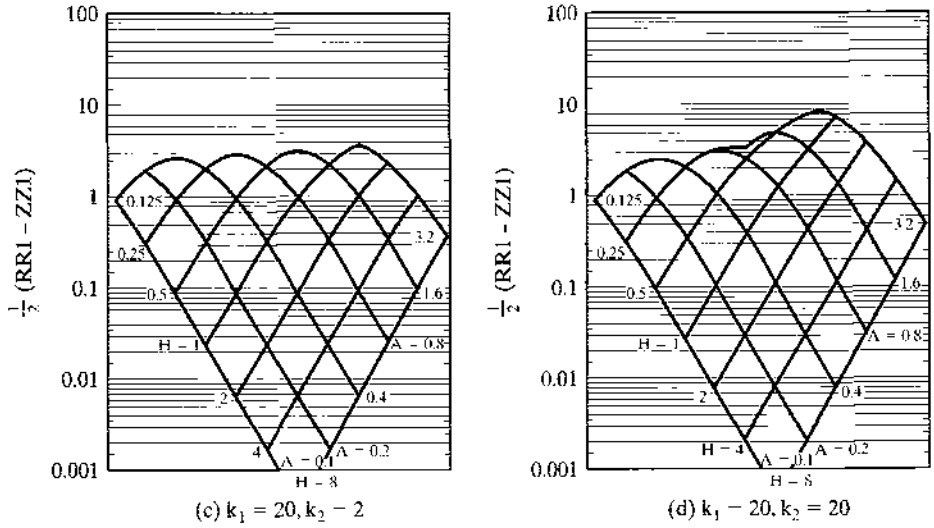

FIGURE 2.31 (Continued)

Example 2.12:

For the same case as Example 2.11, determine the radial strain at the bottom of layer 1, as shown in Figure 2.32. If $h_2 = 8$ in. (203 mm), what is the radial strain at the bottom of layer 1?

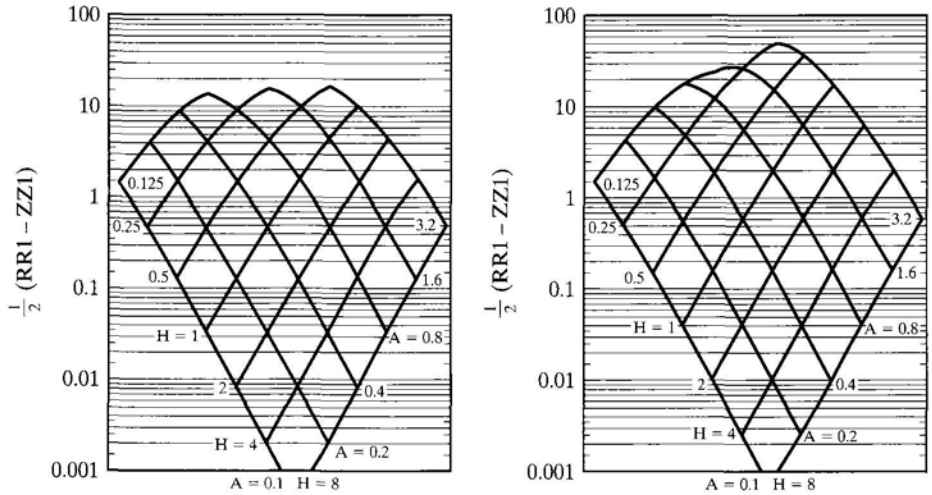

(e) $k_1 = 200, k_2 = 2$ (f) $k_1 = 200, k_2 = 2$

FIGURE 2.31 (Continued)

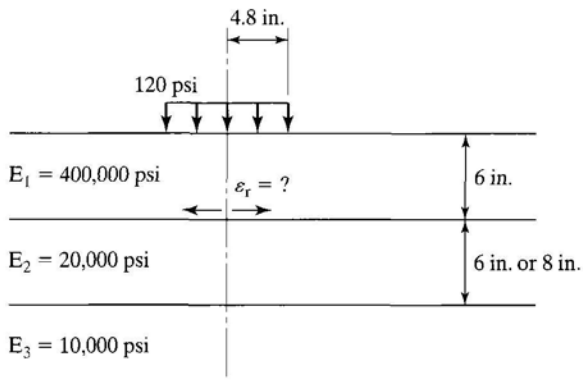

FIGURE 2.32

Example 2.12 (1 in = 25.5 mm, 1 psi = 6.9 kPa).

Solution: Given $k_1 = 20, k_2 = 2, A = 0.8$, and $H = 1.0$, from Figure 2.31*c*, (RR1 − ZZ1)/2 = 1. From Eq. 2.25, $\epsilon_r = 120/400{,}000 = 3 \times 10^{-4}$ (tension), which checks closely with the 2.96×10^{-4} from the table. Given $h_2 = 8$ in. (203 mm), $A = 4.8/8 = 0.6$, and $H = 6/8 = 0.75$, from Figure 2.31*c*, the strain factor is still close to 1, indicating that the thickness of layer 2 has very little effect on the tensile strain due to the predominant effect of layer 1. The radial strain obtained from KENLAYER is 2.91×10^{-4}.

2.3 VISCOELASTIC SOLUTIONS

A viscoelastic material possesses both the elastic property of a solid and the viscous behavior of a liquid. Suppose that a material is formed into a ball. If the ball is thrown on the floor and rebounds, it is said to be elastic. If the ball is left on the table and begins to flow and flatten gradually under its own weight, it is said to be viscous. The viscous component makes the behavior of viscoelastic materials time dependent: the longer the time,

the more the material flows. HMA is a viscoelastic material whose behavior depends on the time of loading, so it is natural to apply the theory of viscoelasticity to the analysis of layered systems. The general procedure is based on the elastic–viscoelastic correspondence principle by applying the Laplace transform to remove the time variable t with a transformed variable p, thus changing a viscoelastic problem to an associated elastic problem. The Laplace inversion of the associated elastic problem from the transformed variable p to the time variable t results in the viscoelastic solutions. Details about the theory of viscoelasticity are presented in Appendix A. A simple collocation method to obtain the viscoelastic solutions from the elastic solutions is presented in this section.

2.3.1 Material Characterization

There are two general methods for characterizing viscoelastic materials: one by a mechanical model, the other by a creep-compliance curve. The latter is used in KENLAYER because of its simplicity. Because Poisson ratio v has a relatively small effect on pavement behavior, it is assumed to be elastic independent of time. Therefore, only modulus E is considered to be viscoelastic and time dependent.

Mechanical Models Figure 2.33 shows various mechanical models for characterizing viscoelastic materials. The models are formed of two basic elements: a spring and a dashpot.

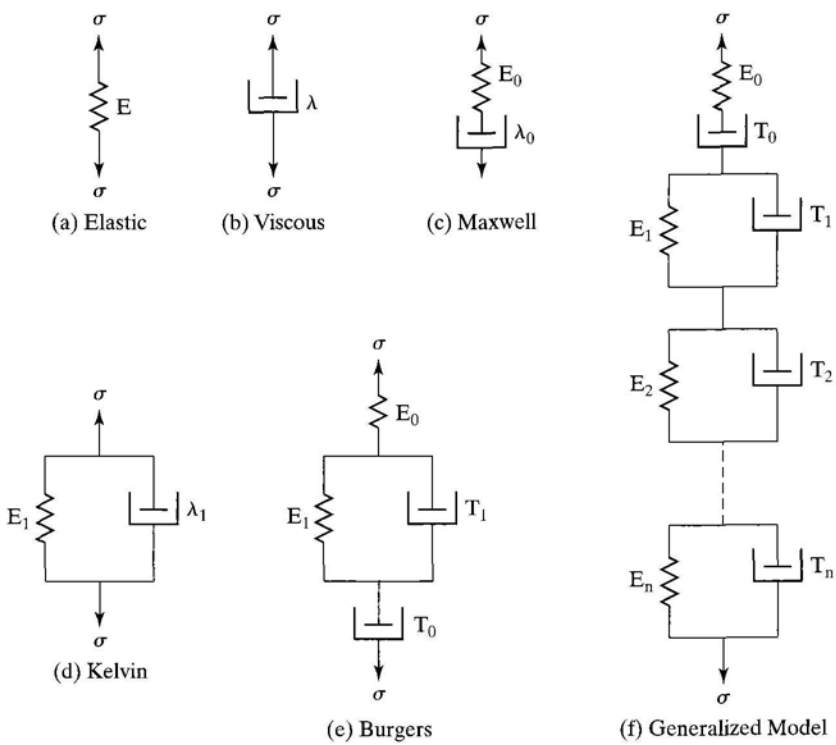

FIGURE 2.33

Mechanical models for viscoelastic materials.

Basic Models An elastic material is characterized by a spring, as indicated in Figure 2.33*a*, and obeys Hooke's law, which asserts that stress is proportional to strain:

$$\sigma = E\epsilon \tag{2.26}$$

Here, σ is stress, ϵ is strain, and E is the elastic modulus.

A viscous material is characterized by a dashpot, as indicated in Figure 2.33*b*, and obeys Newton's law, according to which stress is proportional to the time rate of strain:

$$\sigma = \lambda \frac{\partial \epsilon}{\partial t} \tag{2.27}$$

In this equation, λ is viscosity and t is time. Under a constant stress, Eq. 2.27 can easily be integrated to become

$$\epsilon = \frac{\sigma t}{\lambda} \tag{2.28}$$

Maxwell Model A Maxwell model is a combination of spring and dashpot in series, as indicated in Figure 2.33*c*. Under a constant stress, the total strain is the sum of the strains of both spring and dashpot, or, from Eqs. 2.26 and 2.28,

$$\epsilon = \frac{\sigma}{E_0} + \frac{\sigma t}{\lambda_0} = \frac{\sigma}{E_0}\left(1 + \frac{t}{T_0}\right) \tag{2.29}$$

in which $T_0 = \lambda_0/E_0$ = relaxation time. A subscript 0 is used to indicate a Maxwell model. If a stress σ_0 is applied instantaneously to the model, the spring will experience an instantaneous strain, σ_0/E_0. If this strain is kept constant, the stress will gradually relax and, after a long period of time, will become zero. This can be shown by solving the differential equation

$$\frac{\partial \epsilon}{\partial t} = \frac{1}{E_0}\frac{\partial \sigma}{\partial t} + \frac{\sigma}{\lambda_0} \tag{2.30}$$

The first term on the right side of Eq. 2.30 is the rate of strain due to the spring, the second term that due to the dashpot. If strain is kept constant, $\partial\epsilon/\partial t = 0$, or, after integration,

$$\sigma = \sigma_0 \exp\left(-\frac{t}{T_0}\right) \tag{2.31}$$

It can be seen from Eq. 2.31 that when $t = 0, \sigma = \sigma_0$; when $t = \infty, \sigma = 0$; and when $t = T_0, \sigma = 0.368\,\sigma_0$. Consequently, the relaxation time T_0 of a Maxwell model is the time required for the stress to reduce to 36.8% of the original value. It is more convenient to specify relaxation time than viscosity, because of its physical meaning. A relaxation time of 10 min gives an idea that the stress will relax to 36.8% of the original value in 10 min.

Kelvin Model A Kelvin model is a combination of spring and dashpot in parallel, as indicated in Figure 2.33*d*. Both the spring and the dashpot have the same strain, but the total stress is the sum of the two stresses, or, using subscript 1 to indicate a Kelvin model,

$$\sigma = E_1\epsilon + \lambda_1 \frac{\partial \epsilon}{\partial t}$$

If a constant stress is applied, then

$$\int_0^{\epsilon} \frac{d\epsilon}{\sigma - E_1\epsilon} = \int_0^t \frac{dt}{\lambda_1}$$

or

$$\epsilon = \frac{\sigma}{E_1}\left[1 - \exp\left(-\frac{t}{T_1}\right)\right] \tag{2.32}$$

in which $T_1 = \lambda_1/E_1$ = retardation time. It can be seen from Eq. 2.32 that when $t = 0, \epsilon = 0$; when $t = \infty, \epsilon = \sigma/E_1$, or the spring is fully stretched to its total retarded strain; and when $t = T_1, \epsilon = 0.632\sigma/E_1$. Thus, the retardation time T_1 of a Kelvin model is the time to reach 63.2% of the total retarded strain.

Burgers Model A Burgers model is a combination of Maxwell and Kelvin models in series, as indicated in Figure 2.33*e*. Under a constant stress, from Eqs. 2.29 and 2.32,

$$\epsilon = \frac{\sigma}{E_0}\left(1 + \frac{t}{T_0}\right) + \frac{\sigma}{E_1}\left[1 - \exp\left(-\frac{t}{T_1}\right)\right] \tag{2.33}$$

The total strain is composed of three parts: an instantaneous elastic strain, a viscous strain, and a retarded elastic strain, as shown in Figure 2.34. Qualitatively, a Burgers model well represents the behavior of a viscoelastic material. Quantitatively, a single Kelvin model is usually not sufficient to cover the long period of time over which the retarded strain takes place, and a number of Kelvin models could be needed.

Generalized Model Figure 2.33*f* shows a generalized model that can be used to characterize any viscoelastic material. Under a constant stress, the strain of a generalized model can be written as

$$\epsilon = \frac{\sigma}{E_0}\left(1 + \frac{t}{T_0}\right) + \sum_{i=1}^{n} \frac{\sigma}{E_i}\left[1 - \exp\left(-\frac{t}{T_i}\right)\right] \tag{2.34}$$

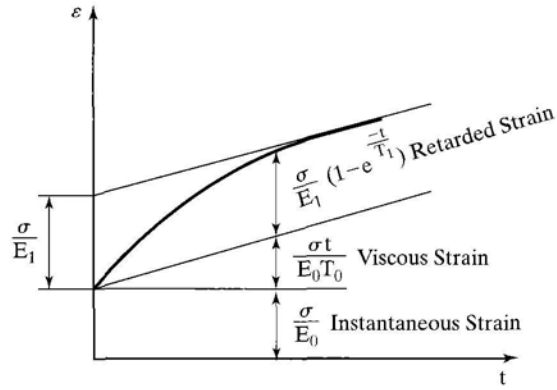

FIGURE 2.34
Three components of strain for a Burgers model.

in which n is the number of Kelvin models. This model explains the effect of load duration on pavement responses. Under a single load application, the instantaneous and the retarded elastic strains predominate, and the viscous strain is negligible. However, under a large number of load repetitions, the accumulation of viscous strains is the cause of permanent deformation.

Creep Compliance Another method to characterize viscoelastic materials is the creep compliance at various times, $D(t)$, defined as

$$D(t) = \frac{\epsilon(t)}{\sigma} \tag{2.35}$$

in which $\epsilon(t)$ is the time-dependent strain under a constant stress.

Under a constant stress, the creep compliance is the reciprocal of Young's modulus. For the generalized model, the creep compliance can be expressed as

$$D(t) = \frac{1}{E_0}\left(1 + \frac{t}{T_0}\right) + \sum_{i=1}^{n} \frac{1}{E_i}\left[1 - \exp\left(-\frac{t}{T_i}\right)\right] \tag{2.36}$$

Given the various viscoelastic constants, E_0, T_0, E_i, and T_i, for a generalized model, the creep compliances at various times can be computed from Eq. 2.36.

Example 2.13:

A viscoelastic material is characterized by one Maxwell model and three Kelvin models connected in series with the viscoelastic constants shown in Figure 2.35*a*. Determine the creep compliance at various times, and plot the creep-compliance curve.

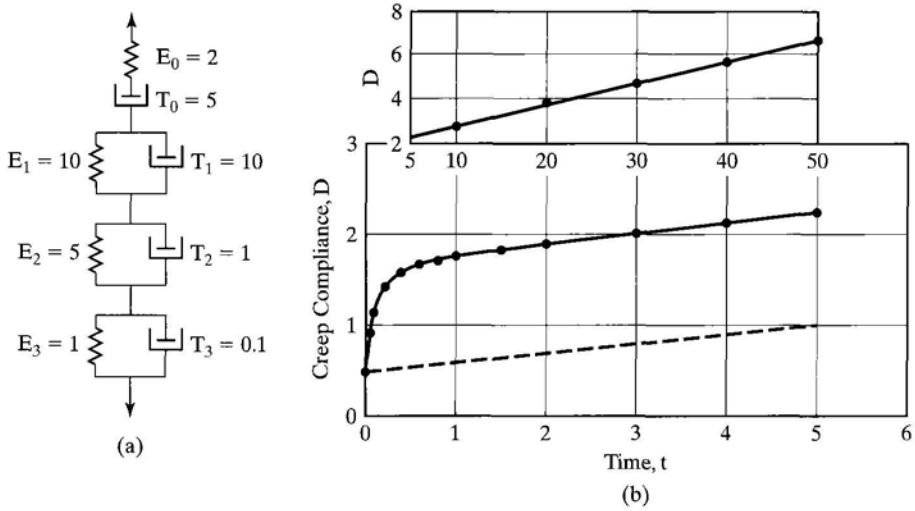

FIGURE 2.35
Example 2.13.

TABLE 2.4 Creep Compliance at Various Times

Time	Creep compliance	Time	Creep compliance
0	0.500	2	1.891
0.05	0.909	3	2.016
0.1	1.162	4	2.129
0.2	1.423	5	2.238
0.4	1.592	10	2.763
0.6	1.654	20	3.786
0.8	1.697	30	4.795
1.0	1.736	40	5.798
1.5	1.819	50	6.799

Solution: In Figure 2.35*a*, no units are given for the viscoelastic constants. If E is in lb/in^2, then the creep compliance is in in.^{2}/lb. If E is in kN/m^2, then the creep compliance is in m^2/kN. If T is in seconds, then the actual time t is also in seconds. From Eq. 2.36, when $t = 0, D = 1/E_0 = \frac{1}{2} = 0.5$; and when $t = 0.1, D = 0.5\,(1 + 0.1/5) + 0.1\,(1 - e^{-0.01}) + 0.2\,(1 - e^{-0.1}) + (1 - e^{-1}) = 1.162$. The creep compliances at various times are tabulated in Table 2.4 and plotted in Figure 2.35*b*. It can be seen that, after $t = 5$, all the retarded strains have nearly completed and only the viscous strains exist, as indicated by a straight line. If the retarded strain lasts much longer, more Kelvin models with longer retardation times will be needed.

If a creep compliance curve is given, the viscoelastic constants of a generalized model can be determined by the method of successive residuals, as described in Appendix A. However, it is more convenient to use an approximate method of collocation, as described below.

2.3.2 Collocation Method

The collocation method is an approximate method to collocate the computed and actual responses at a predetermined number of time durations. Instead of determining both E_i and T_i by the method of successive residuals, several values of T_i are arbitrarily assumed, and the corresponding E_i values are determined by solving a system of simultaneous equations. The method can also be used to obtain the viscoelastic solutions from the elastic solutions.

Elastic Solutions Given the creep compliance of each viscoelastic material at a given time, the viscoelastic solutions at that time can be easily obtained from the elastic solutions, as is illustrated by the following example.

Example 2.14:

Figure 2.36 shows a viscoelastic two-layer system under a circular loaded area having radius 10 in. (254 mm) and uniform pressure 100 psi (690 kPa). The thickness of layer 1 is 10 in. (254 mm), and both layers are incompressible, with Poisson ratio 0.5. The creep compliances of the two materials at five different times are tabulated in Table 2.5. Determine the surface deflection under the center of the loaded area at the given times.

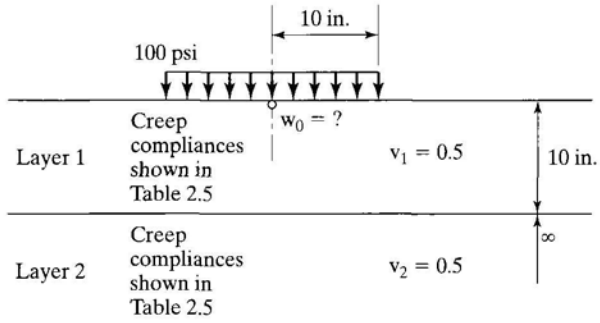

FIGURE 2.36
Example 2.14 (1 in. = 25.4 mm, 1 psi = 6.9 kPa).

Solution: If the modulus ratio is greater than 1, the surface deflection w_0 at any given time can be determined from Figure 2.17. Take $t = 1$ s, for example. The elastic modulus is the reciprocal of creep compliance. For layer 1, $E_1 = 1/(2.683 \times 10^{-6}) = 3.727 \times 10^5$ psi (2.57 GPa) and for layer 2, $E_2 = 1/(19.52 \times 10^{-6}) = 5.123 \times 10^4$ psi (353 MPa), so $E_1/E_2 = 3.727 \times 10^5/(5.123 \times 10^4) = 7.27$. From Figure 2.17, $F_2 = 0.54$, so $w_0 = 1.5 \times 100 \times 10 \times 0.54/(5.123 \times 10^4) = 0.016$ in. (4.1 mm). The same procedure can be applied to other time durations and the results are shown in Table 2.5.

TABLE 2.5 Creep Compliances and Surface Deflections

Time (s)	0.01	0.1	1	10	100
Layer 1 $D(t)$ (10^{-6}/psi)	1.021	1.205	2.683	9.273	18.320
Layer 2 $D(t)$ (10^{-6}/psi)	1.052	7.316	19.520	73.210	110.000
Deflection w_0 (in.)	0.0016	0.0064	0.016	0.059	0.096

Note. 1 psi = 6.9 kPa, 1 in. = 25.4 mm.

It should be noted that the above procedure is not the exact viscoelastic solution. It is a quasi-elastic solution that provides a close approximation to the viscoelastic solution.

Dirichlet Series Pavement design is based on moving loads with a short duration. The creep compliance $D(t)$ caused by the viscous strain is negligible, so Eq. 2.36 can be written as

$$D(t) = \frac{1}{E_0} + \sum_{i=1}^{n} \frac{1}{E_i}\left[1 - \exp\left(-\frac{t}{T_i}\right)\right] \tag{2.37}$$

It is therefore convenient to express the creep compliance as a Dirichlet series, or

$$D(t) = \sum_{i=1}^{n} G_i \exp\left(-\frac{t}{T_i}\right) \tag{2.38}$$

A comparison of Eqs. 2.37 and 2.38 with $T_n = \infty$ shows that

$$G_i = -\frac{1}{E_i} \tag{2.39a}$$

$$G_n = \frac{1}{E_0} + \sum_{i=1}^{n} \frac{1}{E_i} \tag{2.39b}$$

In KENLAYER, the collocation method is applied at two occasions. First, the creep compliances at a reference temperature are specified at a number of time durations and fitted with a Dirichlet series, so that the compliances at any other temperature can be obtained by the time–temperature superposition principle. Second, the elastic solutions obtained at these durations are fitted with a Dirichlet series to be used later for analyzing moving loads.

Collocation of Creep Compliances The creep compliances of viscoelastic materials are determined from creep tests. A 1000-s creep test with compliances measured at 11 different time durations (0.001, 0.003, 0.01, 0.03, 0.1, 0.3, 1, 3, 10, 30 and 100 s) is recommended (FHWA, 1978) to cover all possible range of interest. This range from 0.001 to 100 s should be able to take care of moving loads with both short and long duration as well as the change in creep compliances with temperature.

Because moving loads usually have a very short duration, retardation times T_i of 0.01, 0.03, 0.1, 1, 10, 30, and ∞ seconds are specified in KENLAYER. If creep compliances are specified at seven durations, the coefficients G_1 through G_7 can be determined from Eq. 2.38 by solving 7 simultaneous equations. If the creep compliances are specified at 11 time durations, there are 11 equations but 7 unknowns, so the 11 equations must be reduced to 7 equations by multiplying both sides with a 7 × 11 matrix, which is the transpose of the 11 × 7 matrix, or

$$\begin{bmatrix} \exp\left(-\frac{t_1}{T_1}\right) \ldots \exp\left(-\frac{t_{11}}{T_1}\right) \\ \vdots\ 7 \times 11 \text{ matrix} \ \vdots \\ \exp\left(-\frac{t_1}{T_7}\right) \ldots \exp\left(-\frac{t_{11}}{T_7}\right) \end{bmatrix} \begin{bmatrix} \exp\left(-\frac{t_1}{T_1}\right) \ldots \exp\left(-\frac{t_1}{T_7}\right) \\ \vdots\ 11 \times 7 \text{ matrix} \ \vdots \\ \exp\left(-\frac{t_{11}}{T_1}\right) \ldots \exp\left(-\frac{t_{11}}{T_7}\right) \end{bmatrix} \begin{Bmatrix} G_1 \\ \vdots \\ G_7 \end{Bmatrix}$$

$$= \begin{bmatrix} \exp\left(-\frac{t_1}{T_1}\right) \ldots \exp\left(-\frac{t_{11}}{T_1}\right) \\ \vdots\ 7 \times 11 \text{ matrix} \ \vdots \\ \exp\left(-\frac{t_1}{T_7}\right) \ldots \exp\left(-\frac{t_{11}}{T_7}\right) \end{bmatrix} \begin{Bmatrix} D_1 \\ \vdots \\ D_{11} \end{Bmatrix} \tag{2.40}$$

After coefficients G_1 through G_7 are obtained, the creep compliance at any time t can be computed by Eq. 2.38. The use of 7 equations and 7 unknowns, instead of 11 equations and 11 unknowns, not only saves the computer time but also smooths out the results of creep tests.

Example 2.15:

It is assumed that the creep compliance of a viscoelastic material is represented by

$$D(t) = G_1 \exp(-10t) + G_2 \tag{2.41}$$

If the creep compliances at $t = 0.01$, 0.07, and 0.4 s are 9.516×10^{-5}, 5.034×10^{-4} and 9.817×10^{-4} in.^{2}/lb (13.8, 72.9, and 142.3 mm^2/kN), respectively, determine the coefficients G_1 and G_2.

Solution: With $t_1 = 0.01, t_2 = 0.07, t_3 = 0.4, T_1 = 0.1, T_2 = \infty, D_1 = 9.516 \times 10^{-5}, D_2 = 5.034 \times 10^{-4}$, and $D_3 = 9.817 \times 10^{-4}$. From Eq. 2.40,

$$\begin{bmatrix} e^{-0.1} & e^{-0.7} & e^{-4} \\ 1 & 1 & 1 \end{bmatrix} \begin{bmatrix} e^{-0.1} & 1 \\ e^{-0.7} & 1 \\ e^{-4} & 1 \end{bmatrix} \begin{Bmatrix} G_1 \\ G_2 \end{Bmatrix} = \begin{bmatrix} e^{-0.1} & e^{-0.7} & e^{-4} \\ 1 & 1 & 1 \end{bmatrix} \begin{Bmatrix} 9.516 \times 10^{-5} \\ 5.034 \times 10^{-4} \\ 9.817 \times 10^{-4} \end{Bmatrix}$$

or

$$\begin{bmatrix} 1.066 & 1.420 \\ 1.420 & 3.000 \end{bmatrix} \begin{Bmatrix} G_1 \\ G_2 \end{Bmatrix} = \begin{Bmatrix} 3.541 \times 10^{-4} \\ 1.580 \times 10^{-3} \end{Bmatrix} \tag{2.42}$$

The solution of Eq. 2.42 is $G_1 = -0.001$ in.^{2}/lb (-145 mm^2/kN) and $G_2 = 0.001$ in.^{2}/lb (145 mm^2/kN), which is as expected because the given creep compliances are actually computed from a Kelvin model with

$$D(t) = 0.001\,(1 - e^{-10t}) \tag{2.43}$$

Time–Temperature Superposition It has been demonstrated that asphalt mixes subjected to a temperature increase experience an accelerated deformation as if the time scale were compressed. Figure 2.37 shows the plot of creep compliance D versus time t

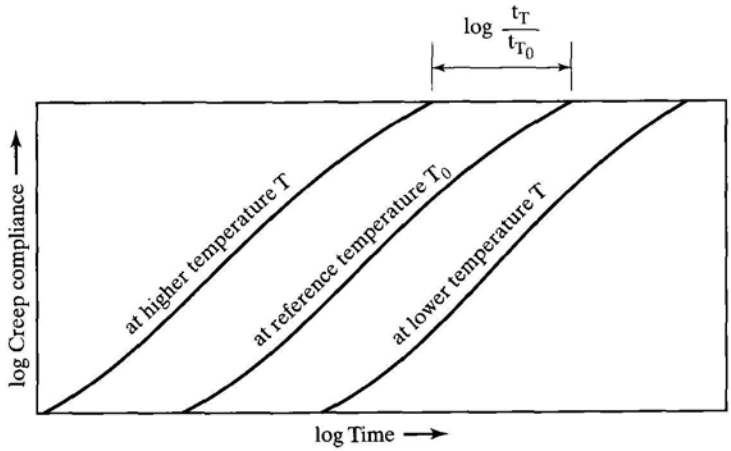

FIGURE 2.37

Creep compliance at different temperatures.

on log scales. At a given time, the creep compliance at a lower temperature is smaller than that at a higher temperature. There is a parallel shift between the curves at various temperatures.

If the creep compliances under a reference temperature T_0 are known, those under any given temperature T can be obtained by using a time–temperature shift factor a_T, defined (Pagen, 1965) as

$$a_T = \frac{t_T}{t_{T_0}} \tag{2.44}$$

in which t_T is the time to obtain a creep compliance at temperature T and t_{T_0} is the time to obtain a creep compliance at reference temperature T_0.

Various laboratory tests on asphalt mixes have shown that a plot of log a_T versus temperature results in a straight line, as shown in Figure 2.38. The slope of the straight line β varies from 0.061 to 0.170, with an average about 0.113 (FHWA, 1978). From Figure 2.38,

$$\beta = \frac{\log(t_T/t_{T_0})}{T - T_0} \tag{2.45}$$

or

$$t_T = t_{T_0} \exp[2.3026\beta(T - T_0)] \tag{2.46}$$

If the creep compliance based on the reference temperature T_0 is

$$D(t) = \sum_{i=1}^{n} G_i \exp\left(-\frac{t_{T_0}}{T_i}\right) \tag{2.47}$$

then the creep compliance based on temperature T is

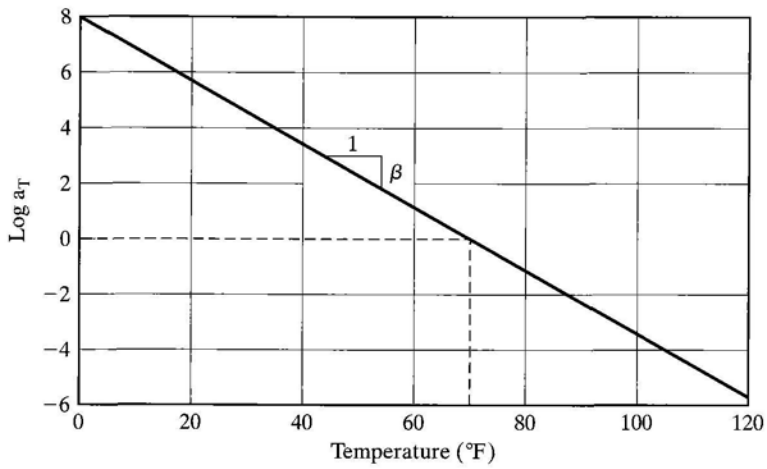

FIGURE 2.38

Shift factor versus temperature.

$$D(t) = \sum_{i=1}^{n} G_i \exp\left(-\frac{t_T}{T_i}\right) \tag{2.48}$$

The relationship between t_T and t_{T_0} is indicated by Eq. 2.46.

Example 2.16:

The expression for the creep compliance at 70°F (21.1°C) is represented by Eq. 2.43. What is the expression for creep compliance at 50°F (10°C) if the time–temperature shift factor β is 0.113?

Solution: From Eq. 2.46, $t_T = t_{T_0} \exp[2.3026 \times 0.113 \times (50 - 70)] = 0.0055 t_{T_0}$. From Eq. 2.43, $D(t) = 0.001[1 - \exp(-0.055t)]$. It can be seen that the creep compliance at 50°F (10°C) is much smaller than that at 70°F (21.1°C).

Collocation for Viscoelastic Solutions Even though the exact viscoelastic solutions is not known, the viscoelastic response R can always be expressed approximately as a Dirichlet series:

$$R = \sum_{i=1}^{7} c_i \exp\left(-\frac{t}{T_i}\right) \tag{2.49}$$

If elastic solutions at 11 time durations are obtained, Eq. 2.40 can be applied to reduce the number of equations to seven, which is the number of unknowns to be solved. If the responses at seven time durations are obtained from the elastic solutions, the coefficients c_1 through c_7 can be solved directly by

$$\begin{bmatrix} e^{-\frac{0.01}{0.01}} & e^{-\frac{0.01}{0.03}} & e^{-\frac{0.01}{0.1}} & e^{-\frac{0.01}{1}} & e^{-\frac{0.01}{10}} & e^{-\frac{0.01}{30}} & 1 \\ e^{-\frac{0.03}{0.01}} & e^{-\frac{0.03}{0.03}} & e^{-\frac{0.03}{0.1}} & e^{-\frac{0.03}{1}} & e^{-\frac{0.03}{10}} & e^{-\frac{0.03}{30}} & 1 \\ e^{-\frac{0.1}{0.01}} & e^{-\frac{0.1}{0.03}} & e^{-\frac{0.1}{0.1}} & e^{-\frac{0.1}{1}} & e^{-\frac{0.1}{10}} & e^{-\frac{0.1}{30}} & 1 \\ e^{-\frac{1}{0.01}} & e^{-\frac{1}{0.03}} & e^{-\frac{1}{0.1}} & e^{-\frac{1}{1}} & e^{-\frac{1}{10}} & e^{-\frac{1}{30}} & 1 \\ e^{-\frac{10}{0.01}} & e^{-\frac{10}{0.03}} & e^{-\frac{10}{0.1}} & e^{-\frac{10}{1}} & e^{-\frac{10}{10}} & e^{-\frac{10}{30}} & 1 \\ e^{-\frac{30}{0.01}} & e^{-\frac{30}{0.03}} & e^{-\frac{30}{0.1}} & e^{-\frac{30}{1}} & e^{-\frac{30}{10}} & e^{-\frac{30}{30}} & 1 \\ 1 & 1 & 1 & 1 & 1 & 1 & 1 \end{bmatrix} \begin{Bmatrix} c_1 \\ c_2 \\ c_3 \\ c_4 \\ c_5 \\ c_6 \\ c_7 \end{Bmatrix} = \begin{Bmatrix} (R)_{0.01} \\ (R)_{0.03} \\ (R)_{0.1} \\ (R)_1 \\ (R)_{10} \\ (R)_{30} \\ (R)_\infty \end{Bmatrix} \tag{2.50}$$

After the coefficients c_i are obtained, the viscoelastic response can be determined by Eq. 2.49.

Example 2.17:

The creep compliance of a homogeneous half-space is expressed as a Dirichlet series shown by Eq. 2.41 with $G_1 = -0.001$ in.^{2}/lb (-145 mm^2/kN), $G_2 = 0.001$ in.^{2}/lb (145 mm^2/kN), $T_1 = 0.1$ s, and $T_2 = \infty$. Assuming that the half-space has Poisson ratio 0.5 and is subjected to a circular load with contact radius 6 in. (152 mm) and contact pressure 80 psi (552 kPa), as shown in Figure 2.39, determine the maximum surface deflection after a loading time of 0.1 s by the collocation method.

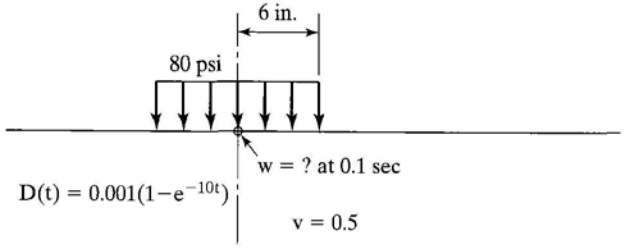

FIGURE 2.39
Example 2.15 (1 in. = 25.4 mm, 1 psi = 6.9 kPa).

Solution: The maximum deflection occurs under the center of the loaded area. With $v = 0.5$, from Eq. 2.8,

$$w_0 = \frac{1.5qa}{E} = 1.5qaD(t) \tag{2.51}$$

Substituting Eq. 2.43 and the values of q and a into Eq. 2.51 yields

$$w_0 = 0.72(1 - e^{-10t}) \tag{2.52}$$

When $t = 0.1$, from Eq. 2.52, then $w_0 = 0.455$ in. (11.6 mm).

The above solution is simple and straightforward. However, to illustrate the collocation method, it is assumed that the surface deflections are expressed as a Dirichlet series, as shown by Eq. 2.49. The elastic response on the right side of Eq. 2.53 is obtained from Eq. 2.52. From Eq. 2.50,

$$\begin{bmatrix} 0.368 & 0.717 & 0.905 & 0.990 & 0.999 & 1.000 & 1 \\ 0.050 & 0.368 & 0.741 & 0.970 & 0.997 & 0.999 & 1 \\ 0.000 & 0.036 & 0.368 & 0.905 & 0.990 & 0.997 & 1 \\ 0.000 & 0.000 & 0.000 & 0.368 & 0.905 & 0.967 & 1 \\ 0.000 & 0.000 & 0.030 & 0.000 & 0.368 & 0.717 & 1 \\ 0.000 & 0.000 & 0.000 & 0.000 & 0.050 & 0.368 & 1 \\ 1 & 1 & 1 & 1 & 1 & 1 & 1 \end{bmatrix} \begin{Bmatrix} c_1 \\ c_2 \\ c_3 \\ c_4 \\ c_5 \\ c_6 \\ c_7 \end{Bmatrix} = \begin{Bmatrix} 0.069 \\ 0.187 \\ 0.455 \\ 0.720 \\ 0.720 \\ 0.720 \\ 0.720 \end{Bmatrix} \tag{2.53}$$

The solution of Eq. 2.53 is $c_1 = 2.186$, $c_2 = -3.260$, $c_3 = 2.214$, $c_4 = -2.055$, $c_5 = 2.446$, $c_6 = -2.229$, and $c_7 = 1.418$. From Eq. 2.49, the surface deflection can be expressed as

$$w_0 = 2.186e^{-t/0.01} - 3.260e^{-t/0.03} + 2.214e^{-t/0.1} - 2.055e^{-t} + 2.446e^{-t/10} - 2.229e^{-t/30} + 1.418 \tag{2.54}$$

When $t = 0.1$, then $w_0 = 0 - 0.116 + 0.814 - 1.859 + 2.422 - 2.222 + 1.418 = 0.457$ in. (11.6 mm), which checks with the exact solution of 0.455 in. (11.6 mm).

2.3.3 Analysis of Moving Loads

The elastic–viscoelastic correspondence principle can be applied directly to moving loads, as indicated by Perloff and Moavenzadeh (1967) for determining the surface deflection of a viscoelastic half-space, by Chou and Larew (1969) for the stresses and displacements in a viscoelastic two-layer system, by Elliott and Moavenzadeh (1971) in a three-layer system, and by Huang (1973b) in a multilayer system. The complexities of the analysis and

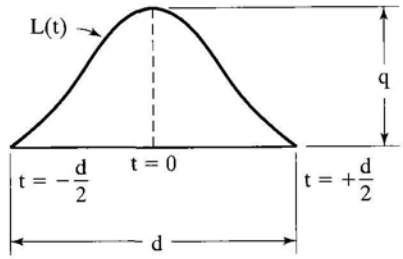

FIGURE 2.40
Moving load as a function of time.

the large amount of computer time required make these methods unsuited for practical use. Therefore, a simplified method has been used in both VESYS and KENLAYER.

In this method, it is assumed that the intensity of load varies with time according to a haversine function, as shown in Figure 2.40. With $t = 0$ at the peak, the load function is expressed as

$$L(t) = q \sin^2\left(\frac{\pi}{2} + \frac{\pi t}{d}\right) \tag{2.55}$$

in which d is the duration of load. When the load is at a considerable distance from a given point, or $t = \pm d/2$, the load above the point is zero, or $L(t) = 0$. When the load is directly above the given point, or $t = 0$, the load intensity is q.

The duration of load depends on the vehicle speed s and the tire contact radius a. A reasonable assumption is that the load has practically no effect when it is at a distance of $6a$ from the point, or

$$d = \frac{12a}{s} \tag{2.56}$$

If $a = 6$ in. and $s = 40$ mph (64 km/h) $= 58.7$ ft/s (17.9 m/s), $d = 0.1$ s.

The response under static load can be expressed as a Dirichlet series:

$$R(t) = \sum_{i=1}^{7} c_i \exp\left(-\frac{t}{T_i}\right) \tag{2.49}$$

The response under moving load can be obtained by Boltzmann's superposition principle:

$$R = \int_{-d/2}^{0} R(t) \frac{dL}{dt} dt \tag{2.57}$$

From Eq. 2.55,

$$\frac{dL}{dt} = -\frac{q\pi}{d} \sin\left(\frac{2\pi t}{d}\right) \tag{2.58}$$

Substituting Eqs. 2.49 and 2.58 into Eq. 2.57 and integrating yields

$$R = \frac{q\pi^2}{2} \sum_{i=1}^{n} c_i \frac{1 + \exp(-d/2T_i)}{\pi^2 + (d/2T_i)^2} \tag{2.59}$$

Example 2.18:

Same as the problem in Example 2.17, but the load is moving at 40 mph (64 km/h). Determine the maximum deflection.

Solution: According to Eq. 2.52 in Example 2.17, the surface deflection under a static load can be expressed as

$$w = 0.72(1 - e^{-10t}) \tag{2.52}$$

The first term is independent of time and therefore remains the same regardless of whether the load is moving. From Eq. 2.59, the second term with $T = 0.1$ and $d = 0.1$ s for 40 mph (64 km/h) should be changed to $0.5 \times \pi^2 \times 0.72\,(1 + e^{-0.5})/(\pi^2 + 0.25) = 0.564$ in. (14.3 mm), so maximum deflection $= 0.72 - 0.564 = 0.156$ in. (3.96 mm).

SUMMARY

This chapter discusses the stresses and strains in flexible pavements and their determinations. An understanding of this subject is indispensable for any mechanistic methods of design.

Important Points Discussed in Chapter 2

1. Boussinesq theory can be applied only to an elastic homogeneous half-space, such as the analysis of a plate bearing test on a subgrade or of a wheel load on a thin pavement.
2. An approximate method to determine the deflection on the surface of a nonlinear elastic half-space, in which the elastic modulus varies with the state of stresses, is to assume the same stress distribution as in the linear theory but vary the moduli according to the state of stresses.
3. The most practical mechanistic method for analyzing flexible pavements is Burmister's layered theory. Based on two-layer elastic systems, various charts were developed for determining pavement responses. The vertical interface stress beneath the center of a circular loaded area can be determined from Figure 2.15, the vertical interface deflection at various radial distances from Figure 2.19. The critical tensile strain at the bottom of layer 1 under a single wheel can be determined from Figure 2.21, under dual wheels from Figure 2.23, and under dual tandem wheels from Figures 2.25, 2.26, and 2.27. For three-layer elastic systems, the stresses and strains at the interfaces beneath the center of a circular loaded area can be determined from Table 2.3 and Figure 2.31.
4. Two methods can be used to characterize viscoelastic materials: a mechanical model and a creep-compliance curve. Both are closely related, and each can be converted to the other. The advantage of using a mechanical model is that the stress–strain relationship can be visualized physically to develop the governing differential equations; the advantage of using a creep-compliance curve is that it can easily be obtained by a laboratory creep test.
5. The elastic–viscoelastic correspondence principle based on Laplace transforms, described in Appendix A, can be used to analyze layered systems consisting of viscoelastic materials. However, a more convenient method is to obtain the elastic solutions at a number of time durations and fit them with a Dirichlet series as a function of time.
6. Instead of using the method of successive residuals, described in Appendix A, a collocation method can be applied to convert the creep compliance to a mechanical model, as indicated by a Dirichlet series. The time–temperature superposition principle, as indicated by Eqs. 2.46 and 2.48, can then be applied to convert the creep compliance from a reference temperature to any given temperature.